CALIBRATION OF A GRATE ON A SLOPING CHANNEL

A THESIS SUBMITTED TO
THE GRADUATE SCHOOL OF NATURAL AND APPLIED SCIENCES
OF
MIDDLE EAST TECHNICAL UNIVERSITY

BY

SABRİ ÖZGÜR SİPAHİ

IN PARTIAL FULFILLMENT OF THE REQUIREMENTS
FOR
THE DEGREE OF MASTER OF SCIENCE
IN
CIVIL ENGINEERING

DECEMBER 2006

Approval of the Graduate School of Natural and Applied Sciences

———————————————

Prof. Dr. Canan Özgen
Director

I certify that this thesis satisfies all the requirements as a thesis for the degree of Master of Science.

———————————————

Prof. Dr. Güney Özcebe
Head of Department

This is to certify that we have read this thesis and that in our opinion it is fully adequate, in scope and quality, as a thesis for the degree of Master of Science.

———————————————

Assist. Prof. Dr. Şahnaz Tiğrek
Supervisor

Examining Committee Members

Prof. Dr. Mustafa Göğüş   (METU,CE)   ———————————————

Assist. Prof. Dr. Şahnaz Tiğrek   (METU,CE)   ———————————————

Prof. Dr. Metin Ger   (METU,CE)   ———————————————

Assoc. Prof. Dr. Zafer Bozkuş   (METU,CE)   ———————————————

Dr. Yurdagül Kumcu   (DSI)   ———————————————

I hereby declare that all information in this document has been obtained and presented in accordance with academic rules and ethical conduct. I also declare that, as required by these rules and conduct, I have fully cited and referenced all material and results that are not original to this work.

Name, Last name :Sabri Özgür SİPAHİ

Signature :

ABSTRACT

CALIBRATION OF A GRATE ON A SLOPING CHANNEL

Sipahi, Sabri Özgür

M.Sc., Department of Civil Engineering

Supervisor: Assist. Prof. Dr. Şahnaz Tiğrek

December 2006, 72 pages

In this study a setup is designed and constructed in the Hydromechanics Laboratory of Middle East Technical University in order to observe the flow through grate inlets under different flow and geometry conditions. The rate of interception of flow is determined over a rectangular channel through preliminary experiments run on the tilting flume. The performance of the new set setup has been examined and grate efficiency is obtained both in terms of longitudinal slope and the Froude number. The results which are obtained show that the setup can be used to conduct experiments to obtain a general expression for grate efficiency.

Key Words: Grate Capacity, Grate Efficiency, Discharge Measurement, Intercepted Flow, Bypass Flow

ÖZ

EĞİMLİ KANALLARDA IZGARA KAPASİTESİNİN KALİBRASYONU

Sipahi, Sabri Özgür

Yüksek Lisans, İnşaat Müh. Bölümü

Tez Danışmanı: Y.Doç. Dr. Şahnaz Tiğrek

Aralık 2006, 72 Sayfa

Bu araştırmada, değişik akım ve geometri koşullarında ızgaradan geçen akımı gözlemek amacıyla yeni bir deney seti tasarlanmış ve inşa edilmiştir. Orta Doğu Teknik Üniversitesi, Hidromekanik Laboratuvarında hazırlanan dikdörtgen, değişken eğimli kanal üzerinde, öncül deneyler yapılarak, ızgaradan geçen akım tespit edilmiştir. Aynı zamanda, deney setinin işlevselliğinin de test edildiği bu çalışmada, ızgara verimi gerek taban eğimi gerekse Froude sayısı'na bağlı olarak ifade edilmiştir. Elde edilen deney sonuçlardan, bu deney setinden, ızgara veriminin genel bir ifadesinin elde edileceği görülmüştür.

Anahtar Kelimeler: Izgara Kapasitesi, Izgara Verimi, Debi Ölçümü, Tutulan Akım, Geçen Akım

ACKNOWLEDGEMENTS

TABLE OF CONTENTS

VIII

LIST OF TABLES

LIST OF FIGURES

LIST OF SYMBOLS

A	: Area
A_R	: Drainage area
C	: Dimensionless runoff coefficient
E	: Efficiency
E_s	: Specific energy
n	: Manning roughness coefficient
Q	: Flow rate
Q_i	: Intercepted flow rate
Q_b	: Bypass flow rate
Q_T	: Total flow rate
Q_R	: Total flow rate in rational formula
Q_1	: Broad-crested weir flow rate
I	: Rainfall intensity
R	: Hydraulic radius
S	: Slope of the channel
Tc	: Time of concentration
y	: Flow depth
y_1	: Upstream flow depth
y_2	: Downstream flow depth
L	: Length
w	: Width
c'	: Bottom rack interception constant
R^2	: Correlation factor

a   : Coefficient of discharge(efficiency) equation

b   : Power coefficient of discharge (efficiency) equation

CHAPTER I

1   INTRODUCTION

1.1   INTRODUCTORY REMARKS

The study of flood prevention and mitigation is a focus in both hydrology and hydraulics. The storm-induced flood is the most severe and frequent natural flood disaster in the world. A rainstorm may generate a large rate of surface runoff in a short period of time in response to high-intensity rainfall. The resulting runoff cannot be drained quickly and leads to water accumulation and flooding in streets, roads and residential areas. Storm drain systems are typically designed to carry flow from a rainfall event away from areas where it is unwanted (such as parking lots and roadways). Flooding occurs when either a heavy storm that exceeds the design criteria of the structure or inadequate capacity. Thus storm water collection system (storm sewers) design is an important part of civil engineering. Storm water collection systems must be properly designed to provide necessary surface drainage and should meet other storm water management goals such as water quality, stream bank channel protection, habitat protection and groundwater recharge.

Storm sewers, in general, can be divided into two categories according to their functions as separate system and combined system. Separate carries only the stormwater from the populated areas. Combined sewers carry water from waste water from residences, offices, industrial complexes, etc during dry periods and convey stormwater during rainfall. This study mainly focuses on the separate system, namely

the stormwater drainage system. The principal or the major hydraulic components in a stormwater drainage system are as follows:

•   Inlet structures that pass runoff from the surface of the land into the closed conduit system,

•   Conduits structures that convey water received from the inlets to other locations,

•   Junctions structures that connect adjacent conduits,

•   Manholes structures that provide ventilation and access for inspection and maintenance, and

•   Outfalls structures that release the runoff into a surface drainage system such as a manmade channel or natural stream.

1.2   HISTORICAL BACKGROUND

The design of stormwater drainage system is generally accomplished by rainfall modeling, runoff modeling, design of conduits and appurtenances. Before designing or evaluating any stormwater drainage system, the engineer must first determine the acceptable level of risk of failure (in the hydrologic sense), which is expressed in the return interval, or the average length of time (in years, taken over a long period of time) between subsequent hydrologic failures. From the return interval, and from an analysis of the contributing watershed, storm duration and depth are determined, from which the discharges that the system must convey are computed.

The development of the Rational equation by Kuichling (1989) and the Manning equation (Manning, 1891) in the late 1880's represents two major advances in modern hydrology. Gradually, hydrologists replaced empiricism with Rational analysis and observed data to solve practical hydrological problems. Green and Ampt (1911) developed a physically based model for infiltration; Sherman (1932) devised the unitgraph (unit hydrograph) method to transform effective rainfall to the direct runoff hydrograph; Horton (1933) developed infiltration theory and a description of

2

drainage basin form (1945); and Gumbel (1941) proposed the extreme value law for hydrologic studies.

Rainfall information can be obtained from a variety of sources, most likely intensity-duration-frequency relations or from rainfall atlases. Once the hyetograph for a design has been developed, it is used to compute runoff rates to be used in the drainage system design. Currently, there are numerous hydrological methods available for computing peak flows, developing runoff hydrographs, and routing hydrographs. Some of them include Rational method, Modified Rational method, SCS/NRCS method, Clark method, Snyder method, Kinematic Wave method, EPA Runoff method and Nash method (Nurünnisa (2001)). The choice and selection of method depends on geographic location, available data, and available resource whether a hydrograph is required or only a peak discharge is needed.

Considering work being conducted for estimating flow to inlets, Beecham and O'Loughlin (1993) have proposed a method which is based on conducted some work on adaptation of the Manning equation guttering systems. The paper by Thomas (1999) introduces several of the practical difficulties involved, such as application to non-uniform gutter profile. Heggen (1984) introduced some further information on guttering technologies. He also included inaccuracies of quotations for the spatially varying flow from Chow, (1959).

Studies focusing on grate inlet interception capacity are rather less in the literature. Woo and Jones (1974) carried out experiments to make suggestions on both the hydraulic capacity and safety of the inlets for bicycle riders by trying inlets with different tilting angles. Kranc and Anderson (1993) have investigated the influence of grates on the overall inlet performance. Brown et al. (1996) listed the grate types for which design procedures were developed. Guo (2000) presented an investigation on street hydraulic capacity. It was found that the street stormwater capacity at a sump is in fact dictated by the storage capacity rather than the conveyance capacity.

1.3   OUTLINE OF THE THESIS

In practical applications, design tables for specific grate types are used in the design stage of drainage systems. In addition standard grate types are used without regarding the flow conditions because of their availability commercially. There exists no specific relationship in the literature that correlates the grate geometry with the interception capacity. In this study a setup is designed and constructed and a grate which can be widely used is selected and the rate of interception of flow by inlet grates is investigated whose results to be used in the design of inlet structures. In Chapter 2 theoretical and mathematical background of the concept is visited. Chapter 3 describes the structuring of the experimental setup and in Chapter 4, experimental findings are presented and the results are interpreted and an equation correlating efficiency and discharge is proposed for using instead of design tables.

CHAPTER II

2 THEORY AND THE METHODOLOGY

Surface drainage of urban roads is an important subject. When an unexpected quantity of rain falls, rainwater cannot be drained easily, and we come across with small lakes in the city centre. For this reason when a sidewalk is made on an urban road, rainwater collected on the bordure should be drained in a suitable way. Horizontal and vertical grates near the sidewalk are used for these reasons. Falling rainwater are collected by the help of grates and manholes and then transmitted to the discharge points by the help of suitable conduits.

The primary purpose of an inlet is to intercept all or a portion of the flow which accumulates in gutters and spread to discharge it into an underground conveyance system. The design characteristics of inlets control the interception and delivery of the flow. Inadequate inlet capacity or poorly located inlets can cause hazardous flooding to the areas which are populated. Therefore, it is the responsibility of the designer is to determine the type, size, and spacing of inlets to intercept a sufficient portion of the gutter flow, while preserving attention to cost. In addition, the designer should ensure that inlets do not project significantly above a pavement surface or pose as an obstacle to traffic.

2.1   INLET STRUCTURES

The primary function of an inlet structure is to allow surface water to enter the storm drainage system. As a secondary function, it serves as access points for cleaning and inspection. The materials most commonly used for inlet construction are cast-in-place concrete and pre-cast concrete. Inlets are typically located in gutter sections, paved medians, and roadside and median ditches. An inlet structure is a box structure with an opening to receive water. An inlet is required at the uppermost point in a gutter section where gutter capacity criteria are violated. This point is established by moving the inlet and thus changing the drainage area until the tributary flow equals the gutter capacity. Inlets are successively spaced to capture flow and the flow from the additional contributing area bypass flow from the previous inlet.

Inlets are also located at intersections to prevent street cross flow. It is desirable to intercept 100 percent of any potential street cross flow. Intersection inlets should be placed on tangent curb sections near corners.

Inlets are also required where the street cross slope begins to superelevate. Sheet flow across the pavement at these locations is particularly susceptible to icing. Inlets should also be located at any point where side drainage enters to the main street and may overload gutter capacity. Where possible, these side drainage inlets should be located to intercept side drainage before it enters the street. Inlets should be placed at all low points in the gutter grade and at median breaks.

2.1.1   Inlet Types

Storm drain inlets are used to collect runoff and discharge it to an underground storm drainage system. Inlets used for the drainage of highway surfaces can be divided into the following four classes (Figure 2.1), (HEC 22, 1991);

6

- grate inlets,
- curb-opening inlets,
- slotted inlets,
- combination inlets.

GRATE INLET

CURB OPENING INLET

SLOTTED DRAIN INLET

COMBINATION INLET
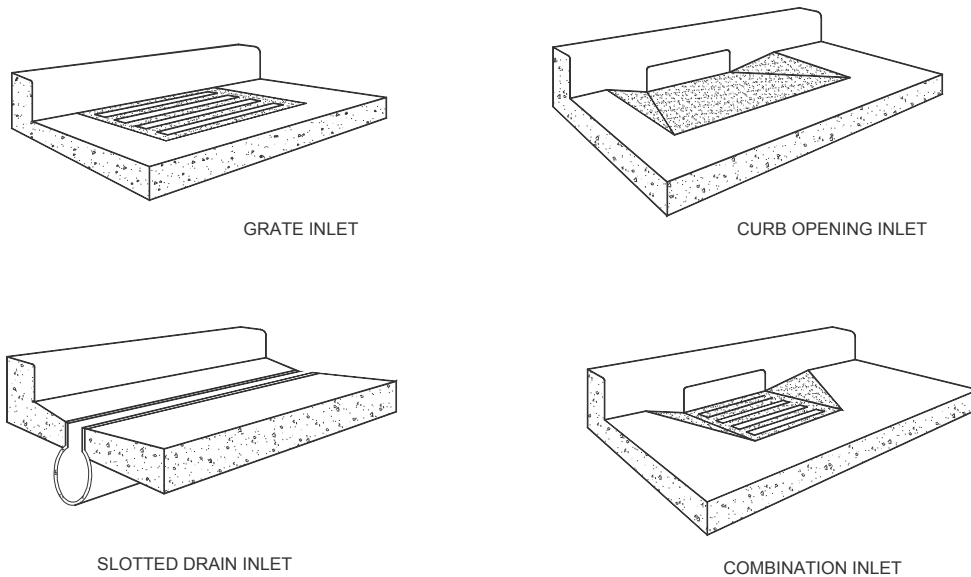
Figure 2.1 Isometric view of grate inlet types

Grate inlets consist of an opening in the gutter. Curb-opening inlets are vertical openings in the curb covered by a top slab. Slotted inlets consist of a pipe cut along the longitudinal axis with bars perpendicular to the opening to maintain the slotted opening. Combination inlets consist of both a curb-opening inlet and a grate inlet placed in a side-by-side configuration, but the curb opening may be located in part upstream of the grate. Slotted drains may also be used with grates and each type of inlet may be installed with or without a depression of the gutter.

Grate inlets, perform satisfactorily over a wide range of gutter grades. Grate inlets generally lose capacity with increase in grade, but to a lesser degree than curb opening inlets. The principal advantage of grate inlets is that they are installed along

the roadway where the water is flowing. Their principal disadvantage is that they may be clogged by floating trash or debris.

2.1.2   Inlet Interception Capacity

Inlet interception capacity is the flow intercepted Q_i, by an inlet under a given set of conditions. The efficiency of an inlet, E, is the percent of total flow that the inlet will intercept for those conditions. The efficiency of an inlet changes with changes in cross slope, longitudinal slope, total gutter flow, and, to a lesser extent, pavement roughness. In mathematical form, efficiency, E, is defined by the following equation:

$$E = \frac{Q_i}{Q_T} \qquad (2.1)$$

where, Q_T is the total gutter flow. Flow that is bypassed, Q_b , is defined as follows:

$$Q_b = Q_T - Q_i \qquad (2.2)$$

The interception capacity of all inlet configurations increases with increasing flow rates, and inlet efficiency generally decreases with increasing flow rates. Factors affecting gutter flow also affect inlet interception capacity. The depth of water next to the curb is the major factor in the interception capacity of both grate inlets and curb-opening inlets. The interception capacity of a grate inlet depends on the amount of water flowing over the grate, the size and configuration of the grate and the velocity of flow in the gutter. The efficiency of a grate is dependent on the same factors of interception capacity and total flow in the gutter. A dimensional analysis which is relating efficiency to flow and geometry properties are given in Appendix C.

2.2   HYDROLOGIC AND HYDRAULIC CONCEPTS

Hydraulic design of storm drainage systems requires an understanding of basic hydrologic and hydraulic concepts and principles. Hydrologic concepts and hydraulic principles will be discussed here.

2.2.1   Hydrologic Concepts

Peak flows are generally adequate for design and analysis of conveyance systems such as storm drains or open channels. However, if the design or analysis must include flood routing (e.g., storage basins or complex conveyance networks), a flood hydrograph is required.

One of the most commonly used equations for the calculation of peak flow from small areas (<10 km^2) is the Rational equation (HEC 22, 1991), it is given as:

$$Q_R = A_R.C.I \tag{2.3}$$

where Q_R is the peak flow, C is the dimensionless runoff coefficient, I is the rainfall intensity and A_R is the drainage area. Intensity is defined as the rate of rainfall and is typically given in units of millimeters per hour.

Assumptions underlying the Rational equation are as follows:

- The peak flow occurs when the entire watershed is contributing to the flow.
- The rainfall intensity is the same over the entire drainage area.
- The rainfall intensity is uniform over the time of concentration, which is the time required for water to travel from the hydraulically most remote point of the basin to the point of focus.
- The frequency of the computed peak flow is the same as that of the rainfall intensity, i.e., the 10-yr. rainfall intensity is assumed to produce the 10-yr.

peak flow.

- The coefficient of runoff is the same for all storms of all recurrence probabilities.

The runoff coefficient, C, in Equation 2.3 is a function of the ground cover and of other hydrologic properties. It relates the estimated peak discharge to a theoretical maximum of 100 percent runoff. Typical values for C are listed in Table 2.1.

Rainfall intensity, duration, and frequency curves (IDF) are necessary for the Rational method. Regional IDF curves are available in most state highway agency manuals, if the IDF curves are not available, they need to be developed.

There are a number of methods that can be used to estimate time of concentration T_c, some of which are intended to calculate the flow velocity within individual segments of the flow path (e.g., shallow concentrated flow, open channel flow, etc.). The time of concentration can be calculated as the sum of the travel times within the various consecutive flow segments.

Table 2.1 Runoff Coefficient C (Mc Ghee, 1991)

TYPE OF SURFACE	C	DESCRIPTION OF AREA	C
Watertight roofs	0.70-0.95	Business (Downtown area)	0.70-0.95
Asphaltic cement streets	0.85-0.90	Business (Neighborhood area)	0.50-0.70
Portland cement streets	0.80-0.95	Urban (Single-family area)	0.30-0.50
Paved driveways and walks	0.75-0.85	Urban (Multi-units, detached)	0.40-0.60
Gravel driveways and walks	0.15-0.30	Urban (Multi-units, attached)	0.60-0.75
Lawns, sandy soil (2% slope)	0.05-0.10	Suburban	0.25-0.40
Lawns, sandy soil (2-7% slope)	0.10-0.15	Apartment areas (Industrial)	0.50-0.70
Lawns, sandy soil (>7% slope)	0.15-0.20	Apartment areas (Light)	0.50-0.80
Lawns, heavy soil (2% slope)	0.13-0.17	Apartment areas (Heavy)	0.60-0.90
Lawns, heavy soil (2-7% slope)	0.18-0.22	Parks, cemeteries	0.10-0.25
Lawns, heavy soil (>7% slope)	0.25-0.35	Playgrounds	0.20-0.35
		Railroad yards	0.20-0.30
		Unimproved areas	0.10-0.30

2.2.2 Hydraulic Concepts

2.2.2.1 Type of Flow and Hydraulic Capacity

The design procedures presented here assume that flow within each storm drain segment is steady and uniform. Also, since storm drain conduits are typically prismatic, the average velocity throughout a segment is considered to be constant.

Two design approaches exist for sizing storm drains under the steady uniform flow assumption. The first is referred to as open channel or gravity flow design. To maintain open channel flow, the segment must be sized so that the water surface within the conduit remains open to atmospheric pressure. If the water surface

throughout the conduit is to be maintained at atmospheric pressure, the flow depth must be less than the height of the conduit. Pressurized flow design requires that the flow in the conduit be at a pressure greater than atmospheric. Under this condition, there is no exposed flow surface within the conduit.

The question of whether open channel or pressurized flow should control design has been debated among various highway agencies. For a given flow rate, larger cross sectional areas (wet area) are required for open channel flow as compared to that for closed conduit flow. It is usually more expensive to construct open channel storm drainage systems. Yet, having a discharge above the design value may be providing additional headroom which is often desirable since the methods of runoff estimation are not exact, and once constructed, storm drains are difficult and expensive to replace. However, there may be situations which require pressurized flow. For example, in some cases, there may be adequate pressurized difference between the conduit axis elevation and inlet/access whole elevation to tolerate pressurized flow. In these cases, significant savings in cost may be realized.

More than often, it is recommended that the storm drains be sized based on a gravity flow criteria at full flow or near full flow condition. Designing for full flow is a conservative assumption since the peak flow actually occurs at 93% of full flow.

The hydraulic capacity of a storm drain is controlled by its size, shape, slope, and friction resistance. Several flow friction equations are available been advanced which define the relationship between flow capacity and these parameters. The most widely used equation for gravity and pressure flow in storm drains is Manning's Equation.

2.2.2.2 Analytical approach to the flow grate inlet

The flow at the grate inlet can be considered as the flow in a channel with bottom rack with parallel bars to the direction of flow as stated in Chow (1959). It is a case of spatially varied flow with decreasing discharge in the flow direction as shown in Figure 2.2 where x denotes the flow direction while y axis is the coordinate axis along the vertical direction.
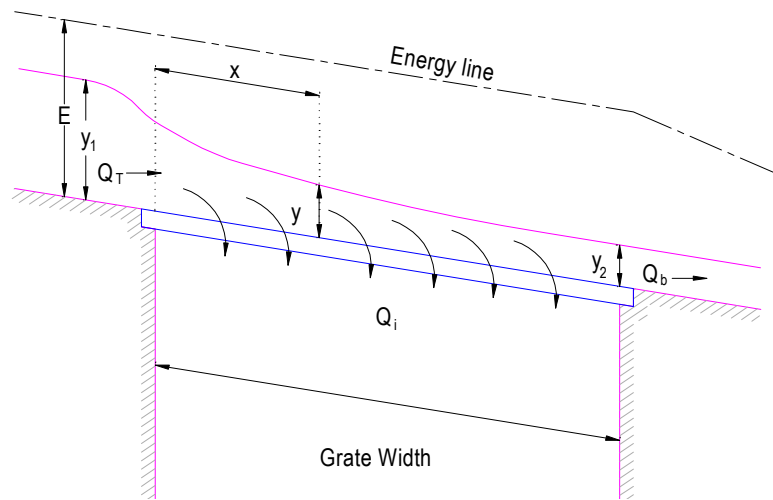
Figure 2.2 Water flowing over the grate

The specific energy at any section of the channel can be written in terms of water depth, y, discharge through the channel, Q, and the width of the channel, w;

$$E_s = y + \frac{Q^2}{2gw^2y^2}$$
(2.4)

From Eq. (2.4), the discharge is

$$Q = wy\sqrt{2g(E_s - y)}$$
(2.5)

The entrance to the reach of the rack described above may be regarded as a broad-crested weir. If the flow over a broad-crested weir is described as:

13

$$Q_1 = c'wE_s^{1.5} \tag{2.6}$$

in which c' may have an average value of 2.80 Chow (1959). Also, Eq. (2.5) gives:

$$Q_T = wy_1\sqrt{2g(E_s - y_1)} \tag{2.7}$$

and

$$Q_b = wy_2\sqrt{2g(E_s - y_2)} \tag{2.8}$$

Thus, the discharge of a partial withdrawal from the main flow through the grate is:

$$Q_i = Q_T - Q_b \tag{2.9}$$

or,

$$Q_i = c'w\left(1 - \frac{y_2\sqrt{E_s - y_2}}{y_1\sqrt{E_s - y_1}}\right)E_s^{1.5} \tag{2.10}$$

The discharge efficiency through the grate varies with longitudinal slope. Efficiency values determined experimentally were found to increase as the longitudinal slope approaches to horizontal slope (Mostkow, 1957). The discharge efficiency increases as the flow depth on the rack increases if the bars are parallel to the direction of the main flow.

2.3   DESIGN METHOD IN TURKEY

The method which is used in Turkey is briefly explained in the following section by regarding the standards from Highways Design Manual (Karayolu Tasarım Elkitabı, 2005).

The basic idea behind the design criteria is to estimate flow gathered over the grate, by considering longitudinal and cross slope geometry of the road. The Rational and Manning Equations are used to estimate the total flow in the gutter and flow depth respectively. The design width of spread is taken from AASTHO and the flow over the grate is assumed to be completely intercepted by the grate used there. Interception capacity of grates is not tested and any grate is placed at a location where spread length is reached to its design value as it is indicated in AASTHO.

Time of the concentration of the rainwater on the surface of road is governed by the cross slope of the road. The relation between time of concentration with the cross slope is as shown in Table 2.2.

Table 2.2 Time of Concentration Table

Cross Slope %	(T_c) Time of concentration (min)
≥5	5
2-5	10
≤2	15

As it is seen from Table 2.2, as the cross slope is increased, time of concentration decreases. This is due to the triangular cross section over the grate. Higher cross section slope results in higher velocities in transverse direction and rainfall accumulates earlier over the grate.

The frequency that is needed to determine the rain intensity is governed by;

- Road safety and the accident probability of a similar road
- Design speed
- Present and future traffic values
- The importance of the road and the potential development of the road location should be considered carefully.

15

On the other hand, the width of water on the pavement depends on;

- Traffic capacity of the road
- Pedestrian volume

CHAPTER III

3   THE EXPERIMENTAL SETUP

The scope of this study is to determine the rate of interception of flow over a channel through experiments run on the tilting flume of the Hydromechanics Laboratory of METU. The specific properties of the experimental setup and details of the experimental procedure are explained in the following sections.

3.1   COMPARISON OF SETUP WITH PRACTICAL USAGE

In this study, zero percent cross slope was used due to the limitations of the setup. However, in practice different cross slopes may be seen. A quick examine to super elevation rates from AASHTO 2001 can easily lead us to conclude that, the cross slope of a road can vary -%10 to +%10.Zero slope can be seen when cross slope changes from negative to positive. When cross slope is different than zero, the flow gathered over the grate has the characteristics of a flow in a triangular channel. On the other hand, pavements and parking lots are the areas where only longitudinal slope is seen. Moreover, due to poor constructions, the cross slope may not be applied in some places. These kinds of places where only longitudinal slope exist have the same conditions with the experimental setup used in this study.

3.2   DEVELOPMENT OF THE EXPERIMENTAL SETUP

A setup is designed to observe the flow through a grate modifying the existing steel channel in the Hydromechanics Laboratory of METU. Necessary modifications for the new setup are explained in detail in the following sections.

3.2.1   Main Channel

A new channel from fiber was implanted in the existing steel channel. The width of the existing channel is 1.00 m. The width of the new fiber glass channel is designed as 0.90m, having 5cm spacing from both sides. The height of the implanted channel is 0.45 m. 0.10 m deep upper portion having a slab constituting the channel simulating the head as depicted in Figure 3.1 and Figure 3.2.
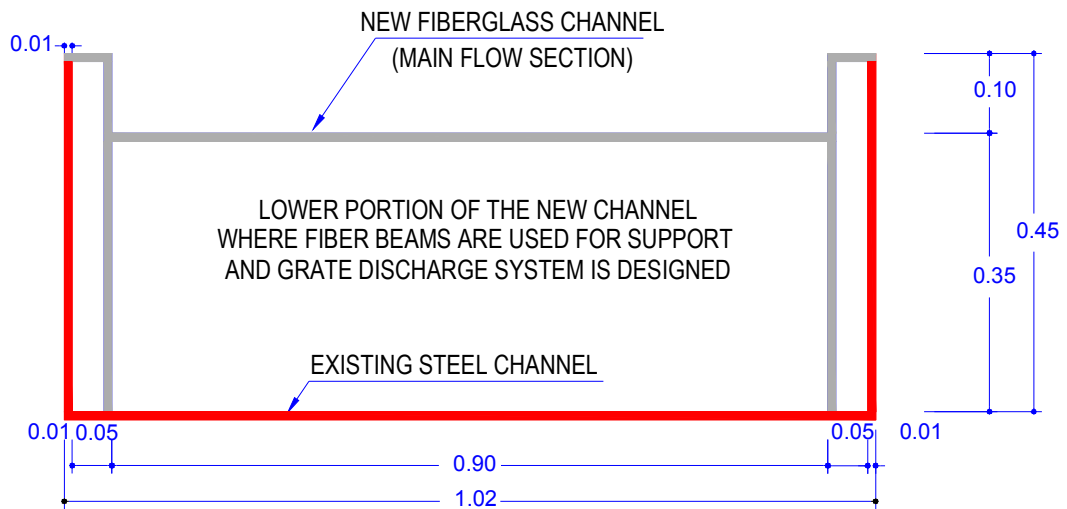
Figure 3.1 Main Channel Section

0.35 m deep lower portion of the channel functions as a supporting base in which 0.01m thick of fiber glasses are placed by 0.25 m spacing forming beams (0.015 m by 0.25 m) to support the slab on it, in order to maintain the surface of the upper channel

straight. Each of 5 beams forms a 1.00 m block constructed as a separate units. After precise measurement of each 1m block in order to form a smooth surface so that water flow is not faced with any obstacle during passage from one to another on the upper channel. After forming the uniform surface, each part is fixed to the existing steel channel. For preventing flow leakage between each 1.00 m portion, special cement is pasted through the slab where two blocks are connected. It should be noted that, the cement used for this purpose is subject to high temperature changes (approximately -20C to +40C), therefore cracks on the cement should be checked regularly and fixed where it is necessary before collecting data from experiments.

Figure 3.2 Upper and lower sections of the channel

3.2.2   Grate Type, Location and Arrangement

The lower and upper part of the channel is designed in the same way for the first 9.00 m of the channel. The 9th meter of the channel is the place, where an inlet is

placed on the upper part to take the water. The location of the first grate is designed to be towards the end of the channel in order to satisfy steady state flow conditions as much as possible. At the location of first grate, the fiber glass support beams form a reservoir for the water taken from the first grate. From the reservoir under the grate, intercepted water is carried with a rectangular discharge channel to the reservoir pool.

The remaining bypassed flow on the upper channel reaches to the location of second grate. In the same way second grate and third grate bypassed flow remains in the upper channel and collected in separate reservoir pool for flow measurement.

Figure 3.3 shows the channel system from the top. Figure 3.4 is a photograph showing general view of the setup.
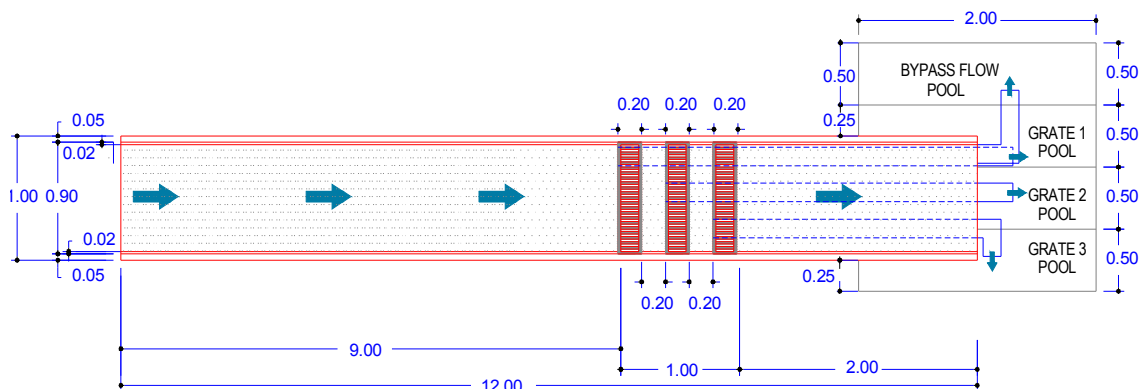
Figure 3.3 Channel System Top View

Figure 3.4 General View of the setup

The geometric characteristic of the grate chosen for the first series is as shown in Figure 3.5. The spacing between the bars of 0.02 m wide is 0.02 m.
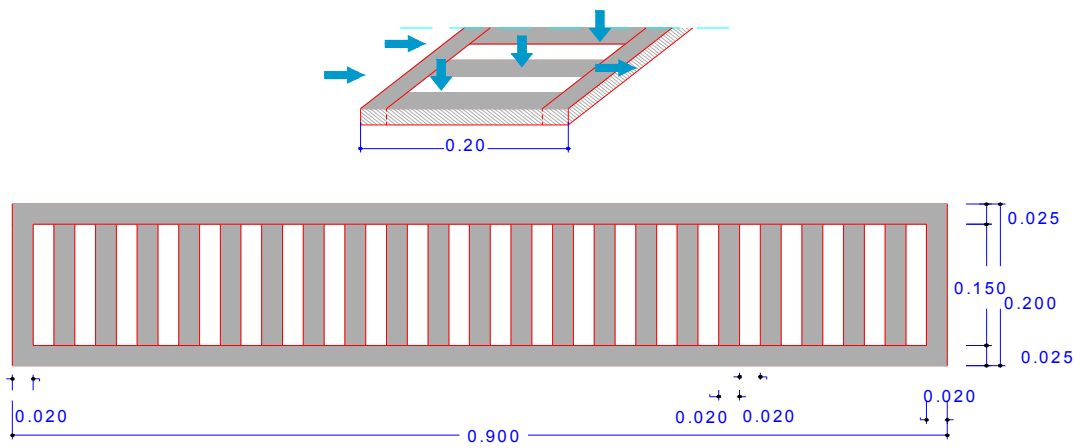
Figure 3.5 Grate Details

Figure 3.6 is a photograph which shows the flow over the grate.

21

Figure 3.6 Flow over the grate

3.2.3 Discharge Channels

In this study only the interception characteristics of the first grate is examined. After this study, first, second and third grates may be used together, one by one or with any other possible combination. Reservoirs for the second and third grate are prepared as well as their discharge channels. The discharge channels of each grate are independent of each other.

The depth of lower portion of the main channel is 0.35 m. In order to place the discharge channel in the lower portion easily, it should be less than 0.35 m in height. The height of the reservoir for the grate inlet must also be taken into account. If 0.90m width of the main channel is with three discharge channels are considered, the width of the discharge channel should be less than 0.30 m. The dimensions of the discharge channels are chosen and arranged as shown in Figures 3.7 and 3.8. All the remaining

space is used for as grate reservoir.
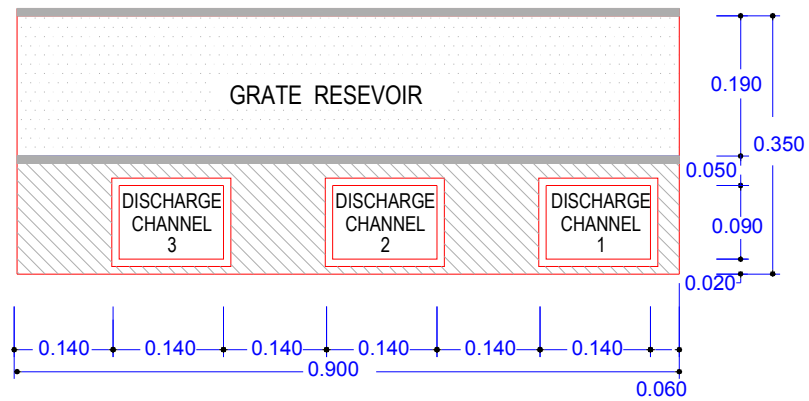
Figure 3.7 Grate Reservoir and Discharge Channels Section
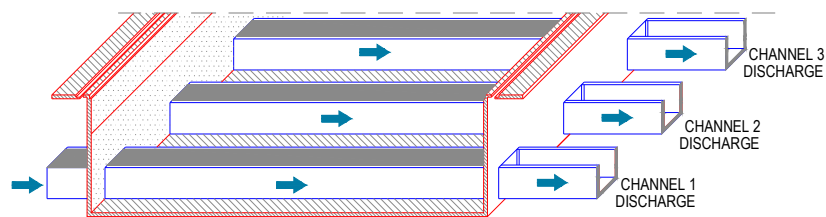
Figure 3.8 Grate Discharge Channels (Isometric View)

Figure 3.8 shows isometric view of grate discharge channels. Figure 3.9 is the photograph which shows grate inlet channels of the setup.

Figure 3.9 Grate Discharge channels

3.2.4 Pools

The collective system was designed to accommodate for three grates operating simultaneously. Therefore, 4 pools are designed just at the end of the channel in order to collect and measure flow from the grates and the bypass flow in the main channel. Pools are constructed from 0.15 m thick fiber glass. Due to the difference in width of

channel and pools, bends are used to divert each flow into the right pool without any splashing to adjacent pool.

The pools are of the size of 2.00, 0.49, 0.60m. Due to the material characteristics of fiber, walls deform due to the pressure of water, especially when the water elevation in a pool is more than 0.30m. The widening of side walls of the pool would change precision of measurements of flow since discharge is measured volumetrically. Moreover, at any time, the fiber walls of the wall would subject to crack and than total failure of the setup. Therefore, rods of thinner fiber glass were used to stiffen the structure. Moreover, a piezometric tube is placed on each pool and a paper with a scale on it is placed just on the wall of the pool at the tube in order to measure the water level in the pool.

From the volume of one pool (0.59 m^3), for the minimum duration of 30 seconds for data collection, maximum value of $0.0197 \text{ m}^3/\text{s}$ of flow can be tested.

For the emptying of the pools, 5.08cm (2 inches) diameter of discharge pipes is placed under each pool. The capacity of the outlet is designed to be higher than the inflow flowing into the pool at maximum flow.

The type of the valve of the pipe is of open-closed one, because it is important to open and close the discharge pipe quickly during experiments. The sketch of the pool and discharge pipe is shown in Figures 3.10 to 3.12.
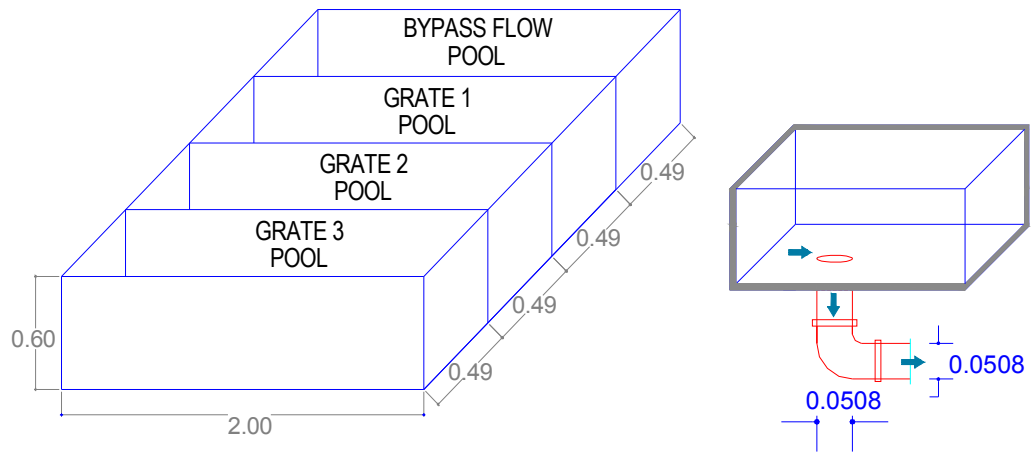
Figure 3.10 Pools and Single Pool discharge system

Figure 3.11 Pools

Figure 3.12 Pool Discharge

3.2.5 Channel Capacity and Rainfall Intensity

It is indicated in section 3.2.1 that, the height of the upper channel is 0.10m. Considering upper channel geometry, the flow capacity of the channel that is tabulated in detail in Tables A.1 to A.6 in the appendix on various slopes is illustrated in Figure 3.13.
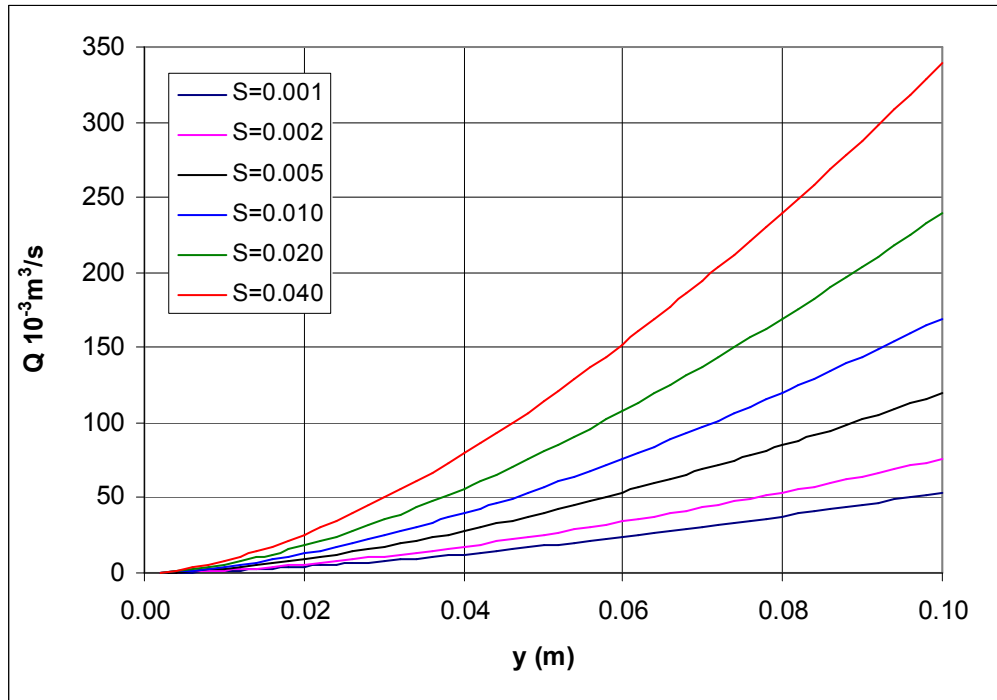
Figure 3.13 Channel Capacity for different slopes

In order to compare the flow capacity of the channel with the flow occurring in daily life, Rational and Manning formulas are used.

$$Q_R = A_R C I \qquad (3.1)$$

A_R is the surface area of the channel up to first grate. Then, if the width of channel (0.90m) is multiplied by length of channel to the first grate (9.0m), A_R is found as 8.1m². Substituting 0.9 as C constant into equation (3.1) and making unit conversions, Q_R can be written as:

$$Q_R = 0.002025I \quad 10^{-3} m^3/s \qquad (3.2)$$

However, in this experiment, total flow is supplied through a constant head instead of rainfall. Therefore, the flow depth on the channel will be calculated by the Manning equation by assuming that the discharge calculated above is equal to the flow in the

channel.

$$Q_R = Q_T = \frac{AR^{2/3}S^{0.5}}{n} \qquad (3.3)$$

Where, S= Slope of the channel, n= Manning roughness coefficient, A is the wetted area and R is the hydraulic radius.

For a rectangular channel, if y is the flow depth and w is the flow width, equation (3.4) is obtained by rearrangement of area and hydraulic radius by means of y and w in equation 3.3 and taking n as 0.010:

$$Q_T = \frac{0.90y\left(\dfrac{0.90y}{2y+0.90}\right)^{2/3}}{0.010}S^{0.5} \qquad (3.4)$$

If equation 3.2 and 3.4 are solved for y, the depth of flow for a specified intensity can be found. For intensity, rainfall, intensity duration, occurrence curves are checked that are obtained from General Directorate of State Meteorology of Turkish Republic (Türkiye Cumhuriyeti Devlet Meteoroloji Genel Müdürlüğü). For instance, if the curve for Hopa (one of the places that highest rainfall is generally seen in Turkey) is examined, the highest rainfall intensity occurring in 5 minutes during 100 year time is about 400 mm/hour. The same value for Ankara is 205 mm/hour, 215 mm/hour for Bodrum, 170 mm/hour for Erzurum, 160 mm/hour for Batman, 210 mm/hour for Siirt, 170 mm/hour for Bolu, 245 mm/ hour for Düzce.

If the rainfall intensity of Hopa is taken, the depths of the flow for six different longitudinal slopes are demonstrated in Table 3.1.

Table 3.1 Height of flow in the channel resulting in 400 mm/hour intensity

S	I (mm/hour)	y (m)	Q 10^{-3}m^3/s
0.040	400	0.00247	0.808
0.020	400	0.00304	0.808
0.010	400	0.00375	0.808
0.005	400	0.00462	0.808
0.002	400	0.00609	0.808
0.001	400	0.00751	0.808

If Table 3.1 and Figure 3.13 are compared, it can be seen that the channel capacity is much higher than the flow representing daily life. The depth of flow resulting in 400mm/hour intensity is less than one centimeter. This situation is the result of the nature of the experimental setup. One is a natural event where rainfall comes from a basin; the other is an experimental setup where water is taken from a constant head tank. In this study, starting from sheet flow, higher depths than illustrated in the above table are tested. The higher depth situation can occur in a flood time or a failure of previous grate inlets in a drainage system which easily seen in daily life.

CHAPTER IV

4   EXPERIMENTAL RESULTS AND DISCUSSIONS

Experiments are carried out at 5 different slopes (S=0, S=1/300, S=1/100, S=1/50, S=1/25) with varying discharges. The total number of the experimental set is 35. Flow regime is subcritical at S=0 and S=1/300, whereas it is supercritical at the remaining slopes. The Froude numbers are 1.74, 1.60, 1.15, 0.63 and 0.48 as the slopes changes from 0 to 1/25.

The measured data are listed in Tables 4.1 to 4.6. In Tables 4.1 to 4.5, the measured total, intercepted and bypass flows rates are given. Error analyses for all measured quantities are given in Appendix B. The data collected were also depicted in Figures 4.1 to 4.5.

Table 4.1 Flow rates observed for S=1/25

Q_T $(10^{-3}m^3/s)$	Intercepted Flow $(10^{-3}m^3/s)$	Bypass Flow $(10^{-3}m^3/s)$
0.25	0.12	0.13
0.89	0.50	0.38
1.59	1.03	0.56
3.37	2.56	0.80
4.91	4.02	0.90

Table 4.2 Flow rates observed for S=1/50

Q_T (10^{-3}m^3/s)	Intercepted Flow (10^{-3}m^3/s)	Bypass Flow (10^{-3}m^3/s)
0.38	0.18	0.19
1.01	0.63	0.39
1.45	1.00	0.44
3.12	2.52	0.59
5.73	4.91	0.82
7.46	6.50	0.96

Table 4.3 Flow rates observed for S=1/100

Q_T (10^{-3}m^3/s)	Intercepted Flow (10^{-3}m^3/s)	Bypass Flow (10^{-3}m^3/s)
0.41	0.23	0.18
1.10	0.74	0.36
1.61	1.19	0.43
2.84	2.34	0.50
4.27	3.76	0.51

Table 4.4 Flow rates observed for S=1/300

Q_T (10^{-3}m^3/s)	Intercepted Flow (10^{-3}m^3/s)	Bypass Flow (10^{-3}m^3/s)
0.22	0.14	0.08
0.43	0.31	0.12
0.82	0.60	0.22
1.18	0.90	0.28
1.55	1.22	0.33
2.20	1.84	0.37
4.27	3.81	0.46

Table 4.5 Flow rates observed for S=0

Q_T $(10^{-3}m^3/s)$	Intercepted Flow $(10^{-3}m^3/s)$	Bypass Flow $(10^{-3}m^3/s)$
0.16	0.10	0.06
0.18	0.11	0.06
0.23	0.16	0.07
0.29	0.20	0.08
0.59	0.43	0.16
0.73	0.55	0.17
0.88	0.68	0.20
1.56	1.27	0.29
1.66	1.38	0.28
2.26	1.92	0.34
2.85	2.51	0.34
4.74	4.29	0.46
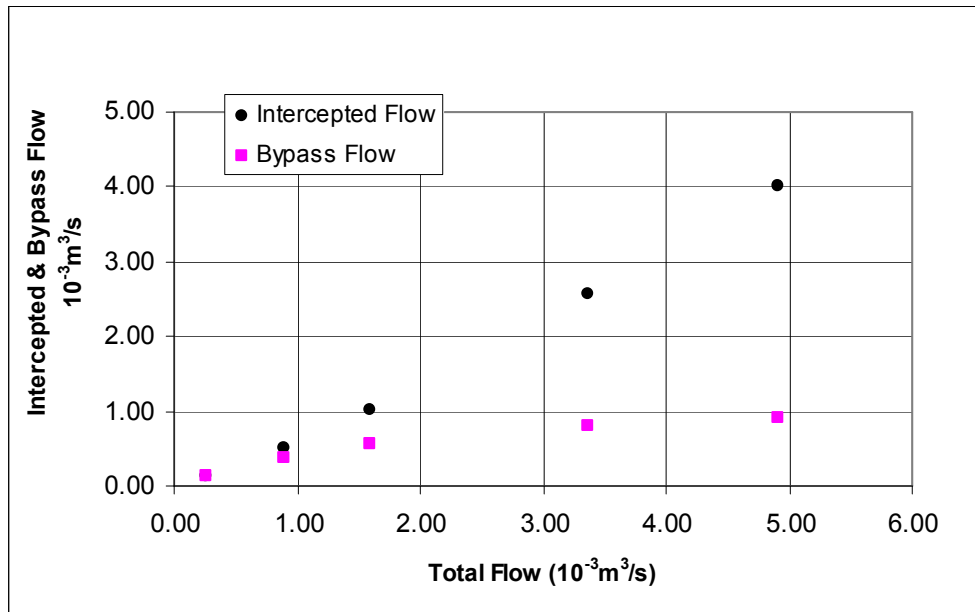
Figure 4.1 Total flow versus Intercepted and Bypass flow for S=1/25
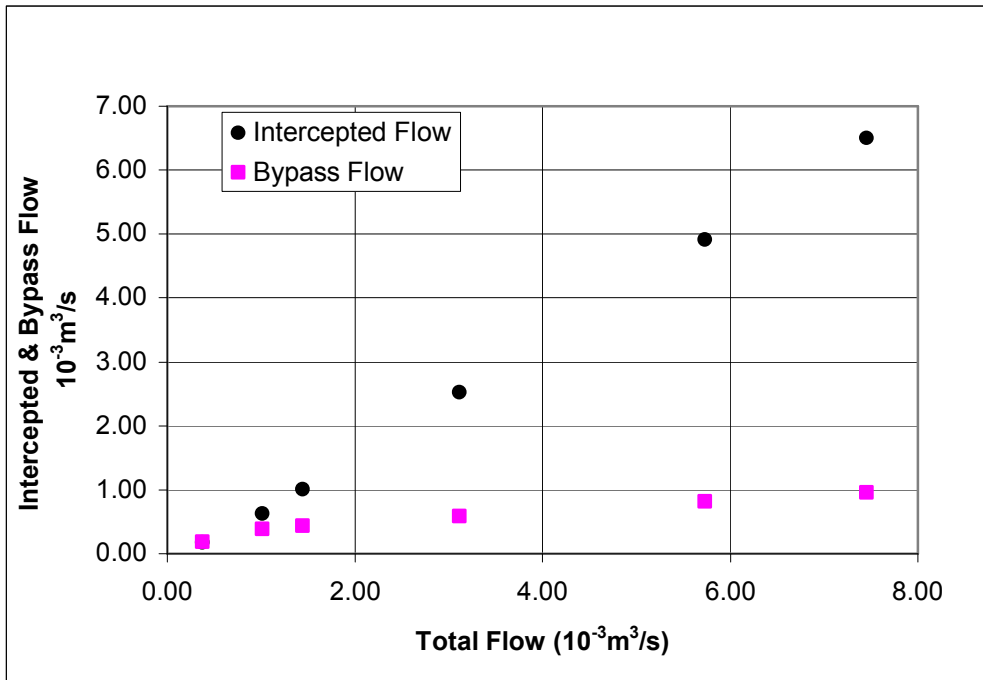
Figure 4.2 Total flow versus Intercepted and Bypass flow for S=1/50
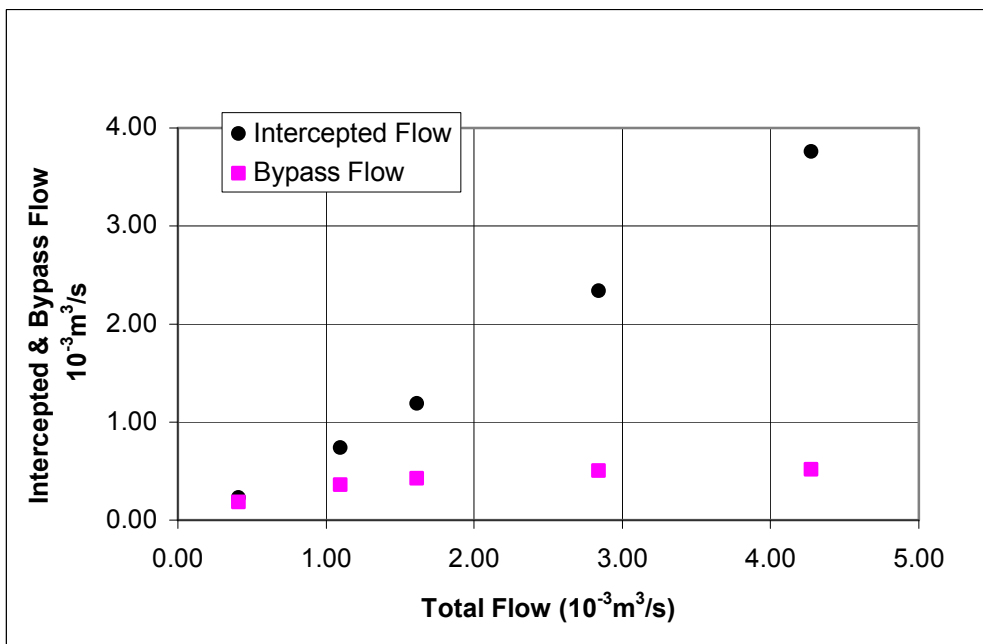
Figure 4.3   Total flow versus Intercepted and Bypass flow for S=1/100
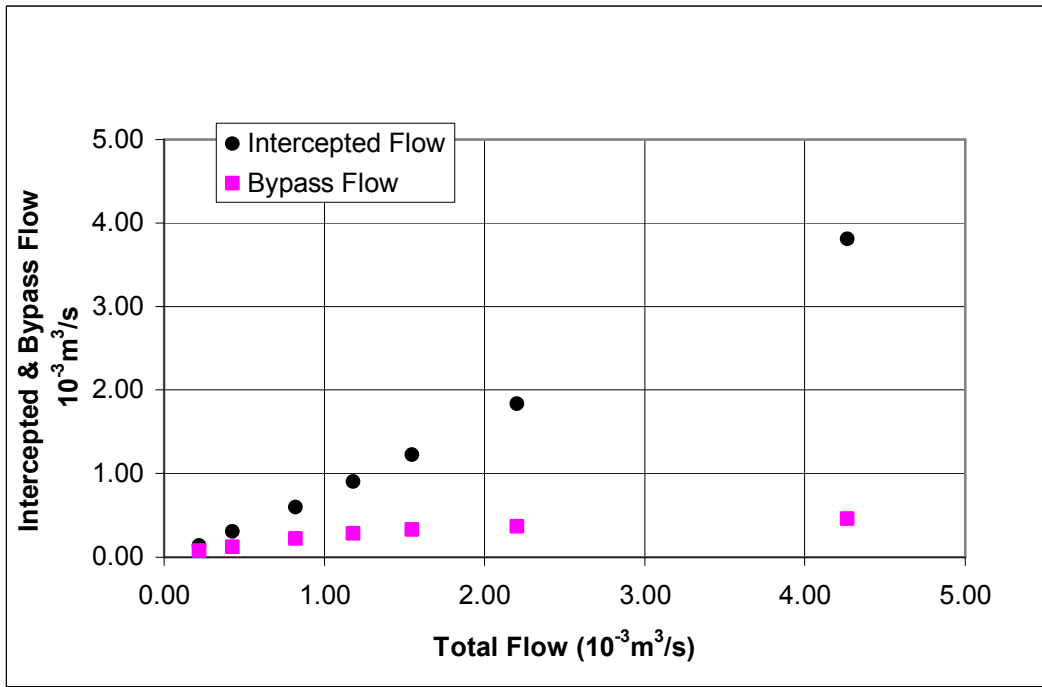
Figure 4.4 Total flow versus Intercepted and Bypass flow for S=1/300
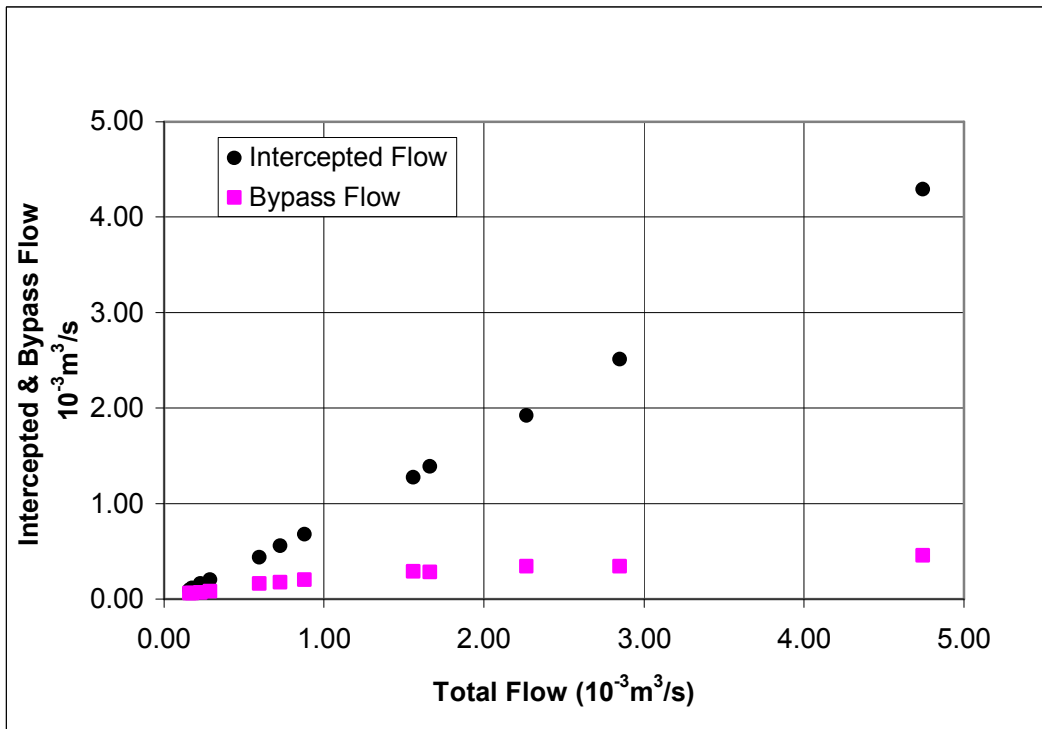
Figure 4.5 Total flow versus Intercepted and Bypass flow for S=0

At the highest flow rate of each slope, upstream and downstream depths on the main channel are also measured and the respective values are given in Table 4.6.

Table 4.6 Upstream and downstream depths for each slope at the highest flow rate

Slope	y_1(m)	y_2 (m)
0	0.023	0.006
1/300	0.018	0.005
1/100	0.012	0.004
1/50	0.014	0.005
1/25	0.010	0.003

4.1   DISCHARGE AND EFFICIENCY

The variation of y, E with S and Q_T is shown in Figures 4.6 to 4.10.
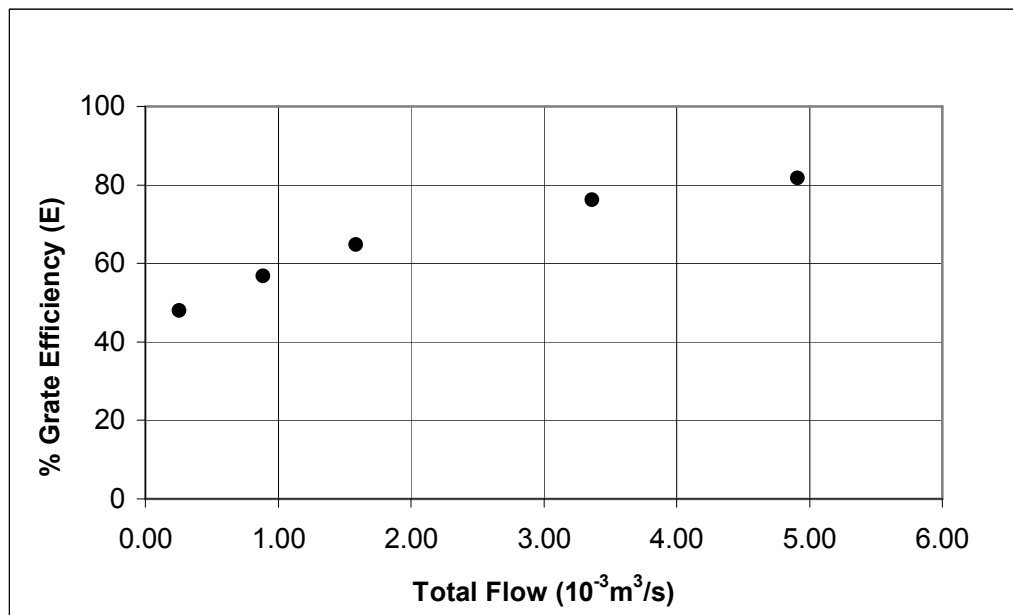
Figure 4.6 Grate efficiency versus Total Flow for S=1/25
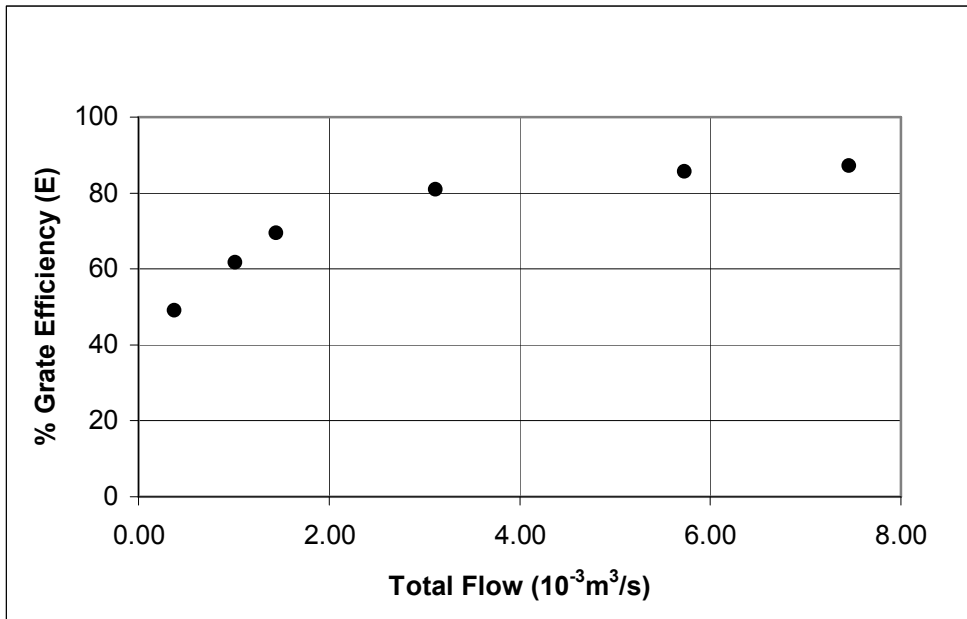
Figure 4.7 Grate efficiency versus Total Flow for S=1/50
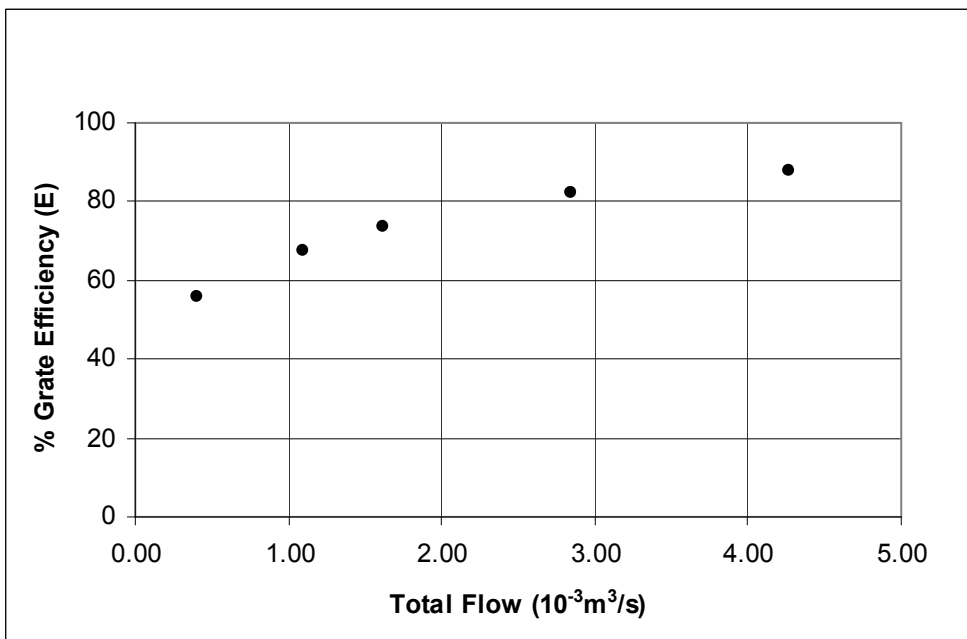
Figure 4.8 Grate efficiency versus Total Flow for S=1/100
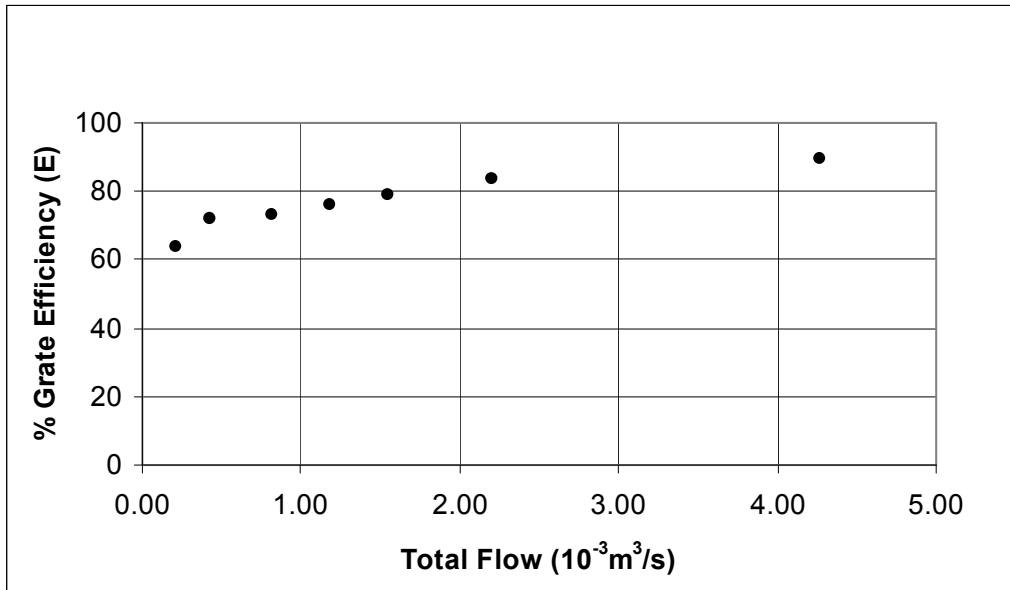
Figure 4.9 Grate efficiency versus Total Flow for S=1/300
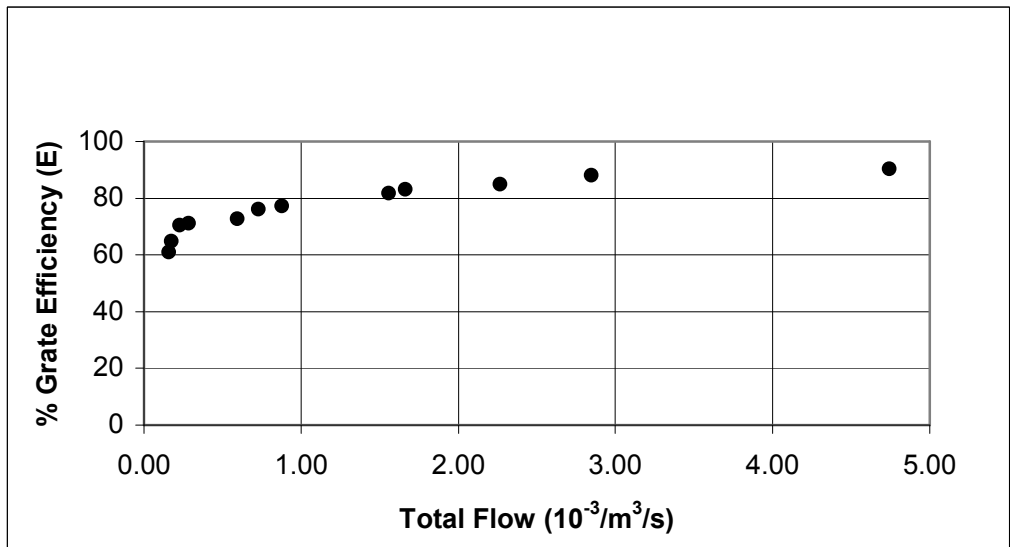
Figure 4.10 Grate efficiency versus Total Flow for S=0

It is observed that there is an increase in the intercepted flow of the grate at higher flow depths. As the flow increased, the ratio of intercepted flow to total flow increased from 40~50% to 80~90% (Figures 4.6 to 4.10). Due to limitations of channel under the grate, higher flow rates could not be tested. As it is stated in Chapter 2, the discharge value increases as the flow depth on the rack increases if the bars are parallel to the direction of the main flow.

When the flow-efficiency relation is checked for grates used in highways, it is seen that efficiency decrease with increasing flows and depths (Hec 22, 1991), (McEnroe, et al (1999)). Actually this result is due to existence of splash over velocity and the width of spread. As the depth increases, due to increasing spread, smaller ratio of water is over the grate. Moreover, due to higher speeds, some water splashes over the grate leading lower ratio of grate interception.

4.2   SLOPE AND EFFICIENCY

In section 4.1, it is shown that, as the flow rate increases, intercepted flow ratio also increases. In order to analyze the behavior of grate efficiency on different slopes, flow rate versus grate efficiencies are plotted together in the same graph (Figure 4.11).
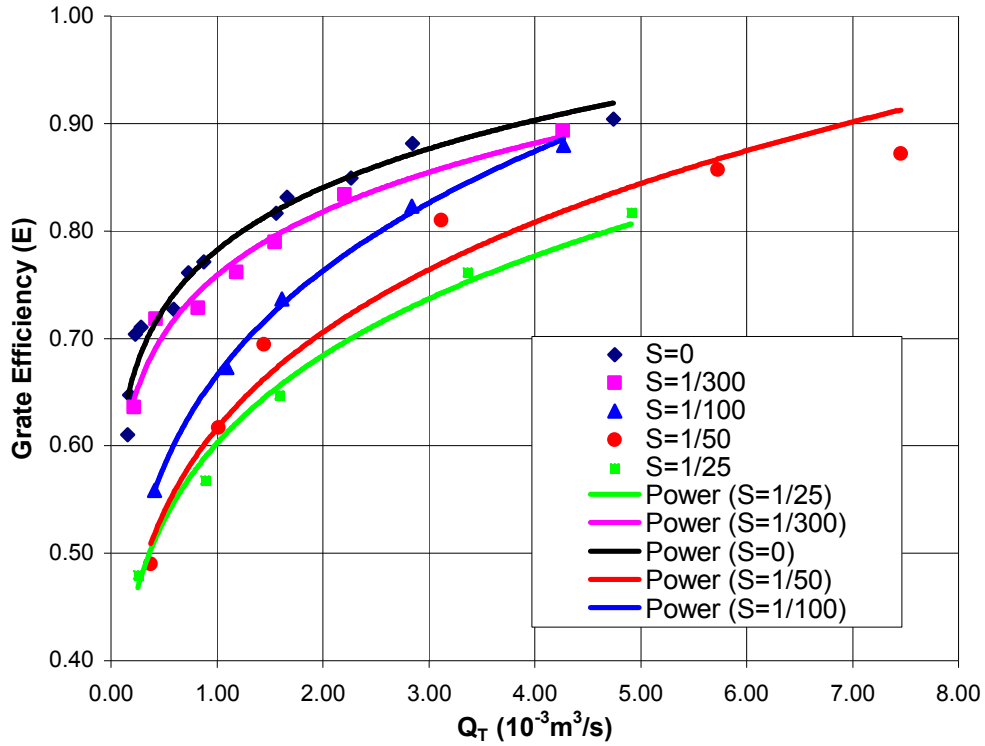
Figure 4.11Grate Efficiency on different slopes with best fitted curves (Power)

From Figure 4.11, it is seen that for a given Q_T the grate efficiency increases as the channel slope approaches to zero. The formula used by power best fitted curves and their R^2 are listed in Table 4.7.

Table 4.7 Comparison of the best fitted curves for efficiency of different slopes

S	Power Trend line Equation	R^2 Power Trend line	Froude Number
1/25	$E = 0.6023Q_T^{0.1835}$	0.9870	1.74
1/50	$E = 0.6163Q_T^{0.1954}$	0.9665	1.60
1/100	$E = 0.6658Q_T^{0.1964}$	0.9985	1.15
1/300	$E = 0.7587Q_T^{0.1084}$	0.9682	0.63
0	$E = 0.7821Q_T^{0.1037}$	0.9536	0.48

If the constants of the each equation listed in Table 4.7 expressed as 'a' and 'b', the general efficiency equation can be written as; $E=a.Q_T^b$. In order to obtain a general equation for grate efficiency, constants 'a' and 'b' is plotted against respective slopes in Figures 4.12 and 4.13.
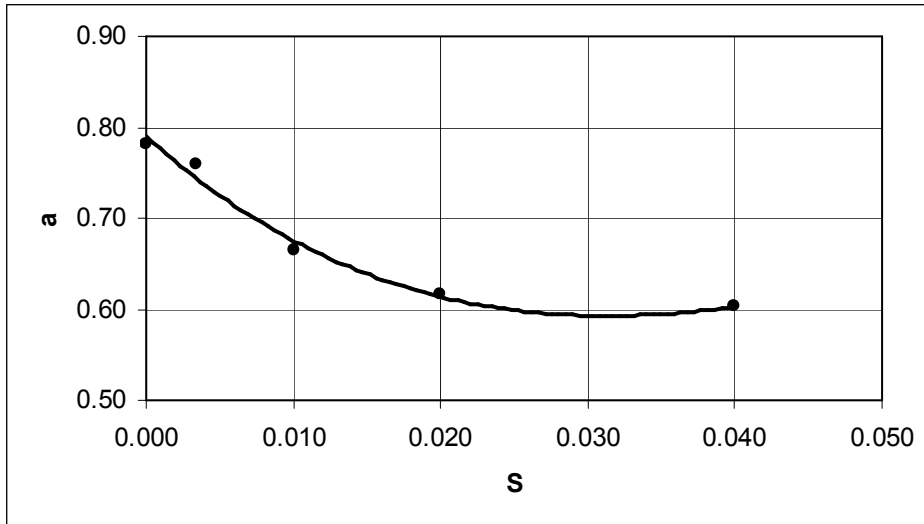
Figure 4.12 Variation of coefficient 'a' (Efficiency equation) with slope
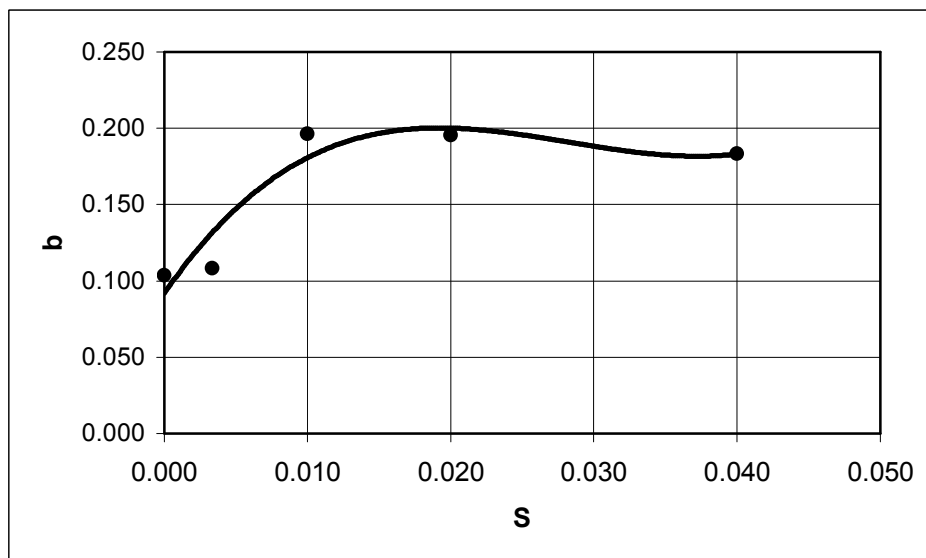
Figure 4.13 Variation of coefficient 'b' (Efficiency equation) with slope

The best fitted curves for a=f(S) and b=f(S) are also plotted in Figures 4.12 and 4.13. The R^2 and equations obtained are listed in Table 4.8.

Table 4.8 Best fitted equation and R^2 of 'a' and 'b' coefficients

	Best fitted Equation	R^2
a	$-1828.848S^3 + 315.679S^2 - 14.366S + 0.789$	0.987
b	$6339.790S^3 - 536.862S^2 + 13.612S + 0.092$	0.894

If the values tabulated in Table 4.8 inserted in $E=aQ_T^{b,}$ the general efficiency equation for the specific grate used in this study is expressed as:

$$E = \left(-1828.848S^3 + 315.679S^2 - 14.366S + 0.789\right)Q_T^{\left(6339.790^3 - 536.862S^2 + 13.612S + 0.092\right)}$$

(4.1)

Since $Q_i = E.Q_T$, equation 4.1 can be revised for Q_i as;

$$Q_i = \left(-1828.848S^3 + 315.679S^2 - 14.366S + 0.789\right)Q_T^{\left(6339.790S^3 - 536.862^2 + 13.612S + 1,092\right)}$$

(4.2)

When calculated Q_i and measured Q_i are compared, the R^2 is found to be 0.999.

The constants 'a' and 'b' defined in efficiency equation in Table 4.7 can also be expressed in terms of the Froude numbers. Froude number dependency is demonstrated in Figures 4.14 and 4.15.
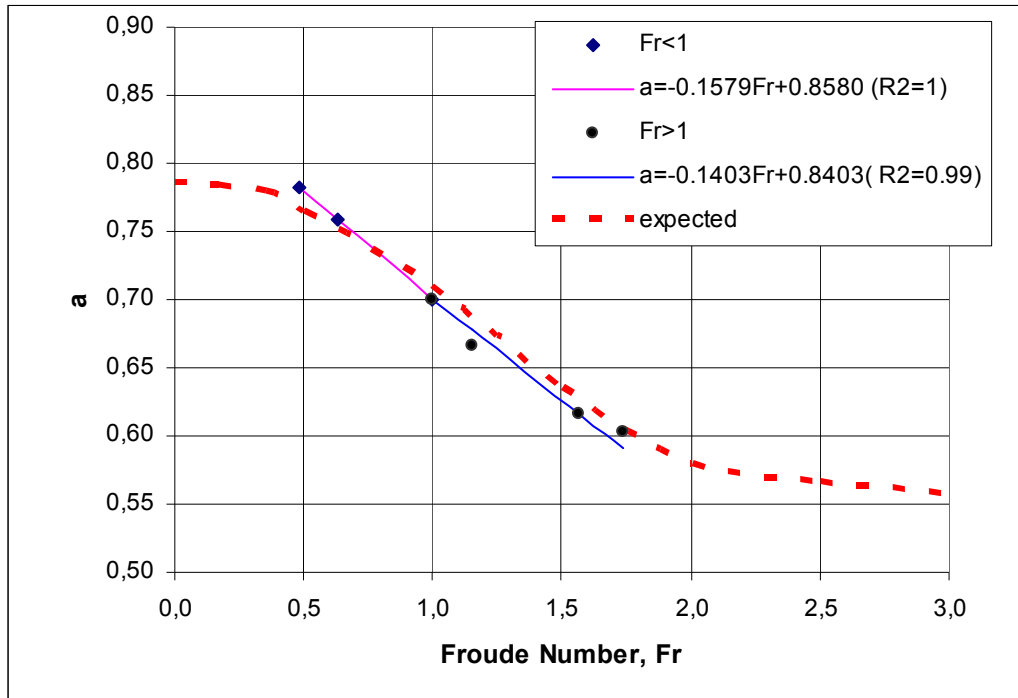
Figure 4.14 Variation of coefficient 'b' (Efficiency equation) with Froude number

Figure 4.15 Variation of coefficient 'b' (Efficiency equation) with Froude number

Both Figure 4.14 and Figure 4.15 are analyzed for subcritical and supercritical regions. The equations of best fitted curves and the boundary conditions for them are listed in Table 4.9.

Table 4.9 Best fitted equation, and R^2 of 'a' and 'b' in terms of Froude numbers

	Best fitted Equation	
a	-0.1579Fr + 0.8580	(for 0.48<Fr<1.00)
a	-0.1403Fr + 0.8403	(for 1.00<Fr<1.74)
b	0.1060	(for 0.48<Fr<1.00)
b	0.1900	(for 1.00<Fr<1.74)

Using the equations listed in Table 4.9, E is expressed as:

$$E = (-0.1579 + 0.8580)Fr(Q_T)^{0.1060} \quad \text{for } 0.48<Fr<1.00 \tag{4.3}$$

$$E = (-0.1403 + 0.8403)Fr(Q_T)^{0.1900} \quad \text{for } 1.00<Fr<1.74 \tag{4.4}$$

In this study, the Froude number changes from 0.48 to 1.74. The best fitted curves are obtained within this range. If higher and lower Froude numbers are considered, the red dashed curves that are sketched in Figures 4.14 and Figure 4.15 are expected rather than best fitted curves obtained in this study.

Increase at the efficiency as the slope of the channel approaches to horizontal is also demonstrated by Mostkow (1957).

The similar results are also seen in cases where cross slope is different from zero percent. The capacity of grates almost increases as the longitudinal slope approaches to zero (Hec 22, 1991), (McEnroe, et al (1999)). In this case, due to horizontal slope, velocity is slower resulting in higher efficiency at horizontal slopes.

4.3   BOTTOM RACK WITHDRAWAL

The upstream and downstream depths measured are sensitive to millimeters. The experimental results are not compared with Equation 2.6 since a change less than one millimeter in flow heights changes the results considerably. In order to make a comparison using Equation 2.6, water depths should be measured with a device having a sensitivity of 0.0001mm. If possible higher water depths should be tested in order to make better analysis for this equation.

4.4   FLOW RATES

During experiments, it is observed that, higher flow rates could be tested if the discharge capacity of the grate were higher. Although the higher rainfall intensity of 5 minutes occurring in a 100 year in Hopa is taken into account in the design of the experimental set-up, it should not be forgotten that, anytime a flood can occur somewhere and a roadway can serve as a river bed. Therefore, in order to test for the flood cases, higher flow depths should be tested.

4.5   GRATE TYPE

Grate interception capacity is another boundary condition for the grate discharge system. At the design stage, a type of grate is chosen as the first stage of this study. As it is seen in Figure 3.5, the spacing between the bars of 0.02 m wide is 0.02 m. If the openings were 0.01 m instead of 0.02 m, higher flow rates could be tested due to decrease in the interception capacity of the grate. Hence discharge system of the grate would serve for higher total flow rates.

4.6   GRATE DISCHARGE

Another boundary condition for higher flow rates is the discharge capacity of the grate system. The dimension of the discharge system together with the grate type governs the maximum total flow in the channel. Larger dimensions of discharge system leads higher flow rates to be tested before choking of water in discharge channel.

CHAPTER V

5   CONCLUSIONS

In the present study, an experimental setup is prepared to test grate interception capacity at different longitudinal slopes and flow rates disregarding cross-slope. During this study the performance of experimental setup is also examined for its usage in future studies. The comparison of the results from literature with the experimental results shows good agreement. Then the following can be concluded:

1. A relationship for the efficiency and hence for the intercepted flow is expressed in terms of total discharge and longitudinal slope.

2. The grate efficiency is affected by the longitudinal slope of the channel. Efficiency or the grate is higher as the longitudinal slope approaches to horizontal.

3. The grate efficiency is also dependent on the total flow flowing through the channel. As flow increases in the channel, the efficiency of the grate increases.

4. In order to compare bottom rack case for grate interception, higher flow rates are required since sensitive measurements of upstream and downstream flow depths are needed.

5. In order to test for higher flow rates, discharge capacity of the grate must be increased or grate type must be changed or more than one grate at a time must be used.

6. In order to make comparative results of grates that are used in highways, cross-slope must be established in the experimental set.

REFERENCES

American Association of State Highway and Transportation Officials, Highway Drainage Guidelines "Vol. IV: Hydraulic Design of Highway Culverts." AASHTO, Inc., Washington, D.C, 1992.

American Society of Civil Engineers, Design Manual for Storm Drainage, New York,1960.

Beecham, S.C and O'Loughlin, G.G. Hydraulics of Spatially Varied Flow in Box Gutters. School of Civil Engineering, University of Technology, Sydney, 1993.

Brown, S. A., S. M. Stein and J. C Warner. 1996. Urban Drainage Design Manual. Hydraulic Engineering Circular No. 22. FHWA-SA-96-278. Washington, D.C. U.S. Department of Transportation, Federal Highway Administration.

Brater, E. F. and H.W. King. Handbook of Hydraulics. 6th ed., McGraw Hill Book Company, New York, NY, 1976

Chow, Ven Te. "Open-Channel Hydraulics", Mc-Graw-Hill, New York, 1959.

Devlet Meteoroloji Genel Müdürlüğü, http://www.meteor.gov.tr , last visited on November 2006

Green, W.H. and G. Ampt. 1911. Studies of soil physics, part I – the flow of air and water through soils. J. Ag. Sci. 4:1-24.

Gumbel, E.J. (1941), 'The Return Period of Flood Flows', Annals of Mathematical Statistics, Vol. 12, pp. 163-90.

Guo, J. C.Y. 2000. Street stormwater storage capacity. Water Environment Research 72: (5) 626-630.

Heggen, Richard J. 1984. Hydraulics of Rainwater Catchment Gutters. University of New Mexico.

Horton, R.E., 1933: The Role of Infiltration in the Hydrological Cycle, Trans. Am. Geophys. Union, Vol.14, pp.446-460.

Horton RE. 1945a. Erosional development of streams and their drainage basins: hydrophysical to quantitative morphology. Bulletin of the Geological Society of America 56: 275-370.

Johnson, F.L. and F.M. Chang, Drainage of Highway Pavements, Hydraulic Engineering Circular No. 12, Federal Highway Administration, Washington, D.C., 1984.

Karayolu Tasarım Elkitabı, Karayolları Genel Müdürlüğü, Ankara, 2005.

Kranc S.C., Anderson M.W. 1993. Investigation of Discharge through Grated Inlets. Final Technical Report, Florida Department of Transportation.

Kuichling, E., 1989: The relation Between the Rainfall and the Discharge of Sewers in Populous Areas, Trans. Of the Amer. Soc. of Civil Eng., 20, pp.1-56.

Manning, R., 1891: On the Flow of Water in Open Channel and Pipes, Trans. Inst. Civil Engrs., Ireland, Vol. 20, pp. 161-207, Dublin, Ireland.

Mc Enroe Bruce M., Wade Reuben P. and Smith Andrew K., HYDRAULIC PERFORMANCE OF CURB AND GUTTER INLETS, K-TRAN: KU-99-1 Final Report, 1999.

Mc Ghee, T.J., 1991. Water Supply and Sewerage, Singapore: Mc Graw Hill.

Mostkow M.A., Sur le calcul des grilles de prise d'eau (Theoretical study of bottom type water intake), La Houille blanche, Grenoble, 12th yr., no, pp. 570-580, September,1957.

Mostkow M.A., "Handbuch der Hydraulic" ("Open-Channel Hydraulics"), VEB Verkag Technic, Berlin, 1956,pp. 204-208 and 213-221.

Noseda G. Operation and design of bottom intake racks, Proceedings of the 6th General Meeting, International Association of Hydraulic Research, The Hague 1955, vol.3, pp. C17-1 to C17-11, 1955.

Nurünnisa Usul, 2001 ENGINEERING HYDROLOGY, Department of Civil Engineering, Middle East Technical University, Ankara-Turkey.

Sherman, L.K., 1932: Streamflow from Rainfall by the Unit-Graph Method, Eng. News Record, 108, pp. 501-505, April.

Thomas, T.H. 1999. Working Paper No. 50 Guttering Design for Rainwater Harvesting.Development Technology Unit.

U.S. Army Corps of Engineers, HEC-22, Urban Drainage Design Manual, Hydrologic Engineering Center, Davis, California,1991.

Woo D.C., Jones S.J., Final Technical Report, Report No: FHWA-RD-74-77, Federal Highway Administration, Washington, 1974.

APPENDIX A

CHANNEL CAPACITY

Channel capacity for the slopes 0.001, 0.002, 0.005, 0.01, 0.02 and 0.04 are given in Tables A1, A2, A3, A4, A5 and A6 respectively.

Table A.1 Channel Capacity for S=0.001

Q 10^{-3}m^3/s	S	n	w (m)	y (m)	A (m^2)	P	R	C	L (m)	Flow Area (m^2)	I (mm/hour)
0.090	0.001	0.01	0.9	0.002	0.002	0.904	0.002	0.9	9	8.1	44
0.285	0.001	0.01	0.9	0.004	0.004	0.908	0.004	0.9	9	8.1	141
0.559	0.001	0.01	0.9	0.006	0.005	0.912	0.006	0.9	9	8.1	276
0.900	0.001	0.01	0.9	0.008	0.007	0.916	0.008	0.9	9	8.1	444
1.302	0.001	0.01	0.9	0.010	0.009	0.920	0.010	0.9	9	8.1	643
1.759	0.001	0.01	0.9	0.012	0.011	0.924	0.012	0.9	9	8.1	869
2.268	0.001	0.01	0.9	0.014	0.013	0.928	0.014	0.9	9	8.1	1120
2.825	0.001	0.01	0.9	0.016	0.014	0.932	0.015	0.9	9	8.1	1395
3.428	0.001	0.01	0.9	0.018	0.016	0.936	0.017	0.9	9	8.1	1693
4.074	0.001	0.01	0.9	0.020	0.018	0.940	0.019	0.9	9	8.1	2012
4.762	0.001	0.01	0.9	0.022	0.020	0.944	0.021	0.9	9	8.1	2352
5.490	0.001	0.01	0.9	0.024	0.022	0.948	0.023	0.9	9	8.1	2711
6.256	0.001	0.01	0.9	0.026	0.023	0.952	0.025	0.9	9	8.1	3089
7.058	0.001	0.01	0.9	0.028	0.025	0.956	0.026	0.9	9	8.1	3486
7.896	0.001	0.01	0.9	0.030	0.027	0.960	0.028	0.9	9	8.1	3899
8.769	0.001	0.01	0.9	0.032	0.029	0.964	0.030	0.9	9	8.1	4330
9.674	0.001	0.01	0.9	0.034	0.031	0.968	0.032	0.9	9	8.1	4777
10.612	0.001	0.01	0.9	0.036	0.032	0.972	0.033	0.9	9	8.1	5240
11.581	0.001	0.01	0.9	0.038	0.034	0.976	0.035	0.9	9	8.1	5719
12.580	0.001	0.01	0.9	0.040	0.036	0.980	0.037	0.9	9	8.1	6212
13.609	0.001	0.01	0.9	0.042	0.038	0.984	0.038	0.9	9	8.1	6720
14.666	0.001	0.01	0.9	0.044	0.040	0.988	0.040	0.9	9	8.1	7243
15.752	0.001	0.01	0.9	0.046	0.041	0.992	0.042	0.9	9	8.1	7779
16.864	0.001	0.01	0.9	0.048	0.043	0.996	0.043	0.9	9	8.1	8328
18.003	0.001	0.01	0.9	0.050	0.045	1.000	0.045	0.9	9	8.1	8891
19.168	0.001	0.01	0.9	0.052	0.047	1.004	0.047	0.9	9	8.1	9466
20.359	0.001	0.01	0.9	0.054	0.049	1.008	0.048	0.9	9	8.1	10054
21.574	0.001	0.01	0.9	0.056	0.050	1.012	0.050	0.9	9	8.1	10654
22.813	0.001	0.01	0.9	0.058	0.052	1.016	0.051	0.9	9	8.1	11266
24.076	0.001	0.01	0.9	0.060	0.054	1.020	0.053	0.9	9	8.1	11890
25.362	0.001	0.01	0.9	0.062	0.056	1.024	0.054	0.9	9	8.1	12525
26.671	0.001	0.01	0.9	0.064	0.058	1.028	0.056	0.9	9	8.1	13171
28.002	0.001	0.01	0.9	0.066	0.059	1.032	0.058	0.9	9	8.1	13828
29.355	0.001	0.01	0.9	0.068	0.061	1.036	0.059	0.9	9	8.1	14496
30.729	0.001	0.01	0.9	0.070	0.063	1.040	0.061	0.9	9	8.1	15175
32.124	0.001	0.01	0.9	0.072	0.065	1.044	0.062	0.9	9	8.1	15864
33.539	0.001	0.01	0.9	0.074	0.067	1.048	0.064	0.9	9	8.1	16562
34.974	0.001	0.01	0.9	0.076	0.068	1.052	0.065	0.9	9	8.1	17271
36.429	0.001	0.01	0.9	0.078	0.070	1.056	0.066	0.9	9	8.1	17990
37.904	0.001	0.01	0.9	0.080	0.072	1.060	0.068	0.9	9	8.1	18718
39.397	0.001	0.01	0.9	0.082	0.074	1.064	0.069	0.9	9	8.1	19455
40.909	0.001	0.01	0.9	0.084	0.076	1.068	0.071	0.9	9	8.1	20202
42.440	0.001	0.01	0.9	0.086	0.077	1.072	0.072	0.9	9	8.1	20958
43.988	0.001	0.01	0.9	0.088	0.079	1.076	0.074	0.9	9	8.1	21722
45.554	0.001	0.01	0.9	0.090	0.081	1.080	0.075	0.9	9	8.1	22496
47.137	0.001	0.01	0.9	0.092	0.083	1.084	0.076	0.9	9	8.1	23278
48.738	0.001	0.01	0.9	0.094	0.085	1.088	0.078	0.9	9	8.1	24068
50.355	0.001	0.01	0.9	0.096	0.086	1.092	0.079	0.9	9	8.1	24867
51.988	0.001	0.01	0.9	0.098	0.088	1.096	0.080	0.9	9	8.1	25673
53.638	0.001	0.01	0.9	0.100	0.090	1.100	0.082	0.9	9	8.1	26488

Table A.2 Channel Capacity for S=0.002

Q 10⁻³m³/s	S	n	w (m)	y (m)	A (m²)	P	R	C	L (m)	Flow Area (m²)	I (mm/hour)
0.127	0.002	0.01	0.9	0.002	0.002	0.904	0.002	0.9	9	8.1	63
0.403	0.002	0.01	0.9	0.004	0.004	0.908	0.004	0.9	9	8.1	199
0.790	0.002	0.01	0.9	0.006	0.005	0.912	0.006	0.9	9	8.1	390
1.273	0.002	0.01	0.9	0.008	0.007	0.916	0.008	0.9	9	8.1	629
1.841	0.002	0.01	0.9	0.010	0.009	0.920	0.010	0.9	9	8.1	909
2.488	0.002	0.01	0.9	0.012	0.011	0.924	0.012	0.9	9	8.1	1228
3.207	0.002	0.01	0.9	0.014	0.013	0.928	0.014	0.9	9	8.1	1584
3.995	0.002	0.01	0.9	0.016	0.014	0.932	0.015	0.9	9	8.1	1973
4.848	0.002	0.01	0.9	0.018	0.016	0.936	0.017	0.9	9	8.1	2394
5.762	0.002	0.01	0.9	0.020	0.018	0.940	0.019	0.9	9	8.1	2845
6.735	0.002	0.01	0.9	0.022	0.020	0.944	0.021	0.9	9	8.1	3326
7.764	0.002	0.01	0.9	0.024	0.022	0.948	0.023	0.9	9	8.1	3834
8.847	0.002	0.01	0.9	0.026	0.023	0.952	0.025	0.9	9	8.1	4369
9.982	0.002	0.01	0.9	0.028	0.025	0.956	0.026	0.9	9	8.1	4929
11.167	0.002	0.01	0.9	0.030	0.027	0.960	0.028	0.9	9	8.1	5515
12.401	0.002	0.01	0.9	0.032	0.029	0.964	0.030	0.9	9	8.1	6124
13.682	0.002	0.01	0.9	0.034	0.031	0.968	0.032	0.9	9	8.1	6756
15.008	0.002	0.01	0.9	0.036	0.032	0.972	0.033	0.9	9	8.1	7411
16.378	0.002	0.01	0.9	0.038	0.034	0.976	0.035	0.9	9	8.1	8088
17.791	0.002	0.01	0.9	0.040	0.036	0.980	0.037	0.9	9	8.1	8786
19.246	0.002	0.01	0.9	0.042	0.038	0.984	0.038	0.9	9	8.1	9504
20.741	0.002	0.01	0.9	0.044	0.040	0.988	0.040	0.9	9	8.1	10243
22.276	0.002	0.01	0.9	0.046	0.041	0.992	0.042	0.9	9	8.1	11001
23.850	0.002	0.01	0.9	0.048	0.043	0.996	0.043	0.9	9	8.1	11778
25.461	0.002	0.01	0.9	0.050	0.045	1.000	0.045	0.9	9	8.1	12573
27.108	0.002	0.01	0.9	0.052	0.047	1.004	0.047	0.9	9	8.1	13387
28.792	0.002	0.01	0.9	0.054	0.049	1.008	0.048	0.9	9	8.1	14218
30.510	0.002	0.01	0.9	0.056	0.050	1.012	0.050	0.9	9	8.1	15067
32.263	0.002	0.01	0.9	0.058	0.052	1.016	0.051	0.9	9	8.1	15932
34.049	0.002	0.01	0.9	0.060	0.054	1.020	0.053	0.9	9	8.1	16814
35.868	0.002	0.01	0.9	0.062	0.056	1.024	0.054	0.9	9	8.1	17713
37.719	0.002	0.01	0.9	0.064	0.058	1.028	0.056	0.9	9	8.1	18627
39.601	0.002	0.01	0.9	0.066	0.059	1.032	0.058	0.9	9	8.1	19556
41.514	0.002	0.01	0.9	0.068	0.061	1.036	0.059	0.9	9	8.1	20501
43.457	0.002	0.01	0.9	0.070	0.063	1.040	0.061	0.9	9	8.1	21460
45.430	0.002	0.01	0.9	0.072	0.065	1.044	0.062	0.9	9	8.1	22434
47.431	0.002	0.01	0.9	0.074	0.067	1.048	0.064	0.9	9	8.1	23423
49.461	0.002	0.01	0.9	0.076	0.068	1.052	0.065	0.9	9	8.1	24425
51.519	0.002	0.01	0.9	0.078	0.070	1.056	0.066	0.9	9	8.1	25441
53.604	0.002	0.01	0.9	0.080	0.072	1.060	0.068	0.9	9	8.1	26471
55.716	0.002	0.01	0.9	0.082	0.074	1.064	0.069	0.9	9	8.1	27514
57.855	0.002	0.01	0.9	0.084	0.076	1.068	0.071	0.9	9	8.1	28570
60.019	0.002	0.01	0.9	0.086	0.077	1.072	0.072	0.9	9	8.1	29639
62.208	0.002	0.01	0.9	0.088	0.079	1.076	0.074	0.9	9	8.1	30720
64.423	0.002	0.01	0.9	0.090	0.081	1.080	0.075	0.9	9	8.1	31814
66.662	0.002	0.01	0.9	0.092	0.083	1.084	0.076	0.9	9	8.1	32920
68.925	0.002	0.01	0.9	0.094	0.085	1.088	0.078	0.9	9	8.1	34037
71.212	0.002	0.01	0.9	0.096	0.086	1.092	0.079	0.9	9	8.1	35167
73.523	0.002	0.01	0.9	0.098	0.088	1.096	0.080	0.9	9	8.1	36308
75.856	0.002	0.01	0.9	0.100	0.090	1.100	0.082	0.9	9	8.1	37460

Table A.3 Channel Capacity for S=0.005

Q 10⁻³m³/s	S	n	w (m)	y (m)	A (m²)	P	R	C	L (m)	Flow Area (m²)	I (mm/hour)
0.201	0.005	0.01	0.9	0.002	0.002	0.904	0.002	0.9	9	8.1	99
0.638	0.005	0.01	0.9	0.004	0.004	0.908	0.004	0.9	9	8.1	315
1.250	0.005	0.01	0.9	0.006	0.005	0.912	0.006	0.9	9	8.1	617
2.013	0.005	0.01	0.9	0.008	0.007	0.916	0.008	0.9	9	8.1	994
2.911	0.005	0.01	0.9	0.010	0.009	0.920	0.010	0.9	9	8.1	1437
3.933	0.005	0.01	0.9	0.012	0.011	0.924	0.012	0.9	9	8.1	1942
5.071	0.005	0.01	0.9	0.014	0.013	0.928	0.014	0.9	9	8.1	2504
6.317	0.005	0.01	0.9	0.016	0.014	0.932	0.015	0.9	9	8.1	3119
7.665	0.005	0.01	0.9	0.018	0.016	0.936	0.017	0.9	9	8.1	3785
9.110	0.005	0.01	0.9	0.020	0.018	0.940	0.019	0.9	9	8.1	4499
10.648	0.005	0.01	0.9	0.022	0.020	0.944	0.021	0.9	9	8.1	5258
12.275	0.005	0.01	0.9	0.024	0.022	0.948	0.023	0.9	9	8.1	6062
13.988	0.005	0.01	0.9	0.026	0.023	0.952	0.025	0.9	9	8.1	6908
15.783	0.005	0.01	0.9	0.028	0.025	0.956	0.026	0.9	9	8.1	7794
17.657	0.005	0.01	0.9	0.030	0.027	0.960	0.028	0.9	9	8.1	8719
19.607	0.005	0.01	0.9	0.032	0.029	0.964	0.030	0.9	9	8.1	9683
21.632	0.005	0.01	0.9	0.034	0.031	0.968	0.032	0.9	9	8.1	10683
23.729	0.005	0.01	0.9	0.036	0.032	0.972	0.033	0.9	9	8.1	11718
25.896	0.005	0.01	0.9	0.038	0.034	0.976	0.035	0.9	9	8.1	12788
28.130	0.005	0.01	0.9	0.040	0.036	0.980	0.037	0.9	9	8.1	13891
30.430	0.005	0.01	0.9	0.042	0.038	0.984	0.038	0.9	9	8.1	15027
32.795	0.005	0.01	0.9	0.044	0.040	0.988	0.040	0.9	9	8.1	16195
35.222	0.005	0.01	0.9	0.046	0.041	0.992	0.042	0.9	9	8.1	17393
37.710	0.005	0.01	0.9	0.048	0.043	0.996	0.043	0.9	9	8.1	18622
40.257	0.005	0.01	0.9	0.050	0.045	1.000	0.045	0.9	9	8.1	19880
42.862	0.005	0.01	0.9	0.052	0.047	1.004	0.047	0.9	9	8.1	21166
45.524	0.005	0.01	0.9	0.054	0.049	1.008	0.048	0.9	9	8.1	22481
48.241	0.005	0.01	0.9	0.056	0.050	1.012	0.050	0.9	9	8.1	23823
51.012	0.005	0.01	0.9	0.058	0.052	1.016	0.051	0.9	9	8.1	25191
53.836	0.005	0.01	0.9	0.060	0.054	1.020	0.053	0.9	9	8.1	26586
56.712	0.005	0.01	0.9	0.062	0.056	1.024	0.054	0.9	9	8.1	28006
59.639	0.005	0.01	0.9	0.064	0.058	1.028	0.056	0.9	9	8.1	29451
62.615	0.005	0.01	0.9	0.066	0.059	1.032	0.058	0.9	9	8.1	30921
65.639	0.005	0.01	0.9	0.068	0.061	1.036	0.059	0.9	9	8.1	32414
68.712	0.005	0.01	0.9	0.070	0.063	1.040	0.061	0.9	9	8.1	33932
71.831	0.005	0.01	0.9	0.072	0.065	1.044	0.062	0.9	9	8.1	35472
74.995	0.005	0.01	0.9	0.074	0.067	1.048	0.064	0.9	9	8.1	37035
78.205	0.005	0.01	0.9	0.076	0.068	1.052	0.065	0.9	9	8.1	38620
81.459	0.005	0.01	0.9	0.078	0.070	1.056	0.066	0.9	9	8.1	40227
84.756	0.005	0.01	0.9	0.080	0.072	1.060	0.068	0.9	9	8.1	41855
88.095	0.005	0.01	0.9	0.082	0.074	1.064	0.069	0.9	9	8.1	43504
91.476	0.005	0.01	0.9	0.084	0.076	1.068	0.071	0.9	9	8.1	45173
94.898	0.005	0.01	0.9	0.086	0.077	1.072	0.072	0.9	9	8.1	46863
98.360	0.005	0.01	0.9	0.088	0.079	1.076	0.074	0.9	9	8.1	48573
101.862	0.005	0.01	0.9	0.090	0.081	1.080	0.075	0.9	9	8.1	50302
105.402	0.005	0.01	0.9	0.092	0.083	1.084	0.076	0.9	9	8.1	52050
108.981	0.005	0.01	0.9	0.094	0.085	1.088	0.078	0.9	9	8.1	53818
112.597	0.005	0.01	0.9	0.096	0.086	1.092	0.079	0.9	9	8.1	55603
116.250	0.005	0.01	0.9	0.098	0.088	1.096	0.080	0.9	9	8.1	57407
119.939	0.005	0.01	0.9	0.100	0.090	1.100	0.082	0.9	9	8.1	59229

Table A.4 Channel Capacity for S=0.01

Q 10^{-3}m^3/s	S	n	w (m)	y (m)	A (m^2)	P	R	C	L (m)	Flow Area (m^2)	I (mm/hour)
0.285	0.01	0.01	0.9	0.002	0.002	0.904	0.002	0.9	9	8.1	141
0.902	0.01	0.01	0.9	0.004	0.004	0.908	0.004	0.9	9	8.1	445
1.767	0.01	0.01	0.9	0.006	0.005	0.912	0.006	0.9	9	8.1	873
2.846	0.01	0.01	0.9	0.008	0.007	0.916	0.008	0.9	9	8.1	1406
4.117	0.01	0.01	0.9	0.010	0.009	0.920	0.010	0.9	9	8.1	2033
5.562	0.01	0.01	0.9	0.012	0.011	0.924	0.012	0.9	9	8.1	2747
7.171	0.01	0.01	0.9	0.014	0.013	0.928	0.014	0.9	9	8.1	3541
8.933	0.01	0.01	0.9	0.016	0.014	0.932	0.015	0.9	9	8.1	4411
10.839	0.01	0.01	0.9	0.018	0.016	0.936	0.017	0.9	9	8.1	5353
12.884	0.01	0.01	0.9	0.020	0.018	0.940	0.019	0.9	9	8.1	6362
15.059	0.01	0.01	0.9	0.022	0.020	0.944	0.021	0.9	9	8.1	7437
17.360	0.01	0.01	0.9	0.024	0.022	0.948	0.023	0.9	9	8.1	8573
19.782	0.01	0.01	0.9	0.026	0.023	0.952	0.025	0.9	9	8.1	9769
22.320	0.01	0.01	0.9	0.028	0.025	0.956	0.026	0.9	9	8.1	11022
24.970	0.01	0.01	0.9	0.030	0.027	0.960	0.028	0.9	9	8.1	12331
27.729	0.01	0.01	0.9	0.032	0.029	0.964	0.030	0.9	9	8.1	13693
30.593	0.01	0.01	0.9	0.034	0.031	0.968	0.032	0.9	9	8.1	15108
33.558	0.01	0.01	0.9	0.036	0.032	0.972	0.033	0.9	9	8.1	16572
36.622	0.01	0.01	0.9	0.038	0.034	0.976	0.035	0.9	9	8.1	18085
39.782	0.01	0.01	0.9	0.040	0.036	0.980	0.037	0.9	9	8.1	19645
43.035	0.01	0.01	0.9	0.042	0.038	0.984	0.038	0.9	9	8.1	21252
46.379	0.01	0.01	0.9	0.044	0.040	0.988	0.040	0.9	9	8.1	22903
49.811	0.01	0.01	0.9	0.046	0.041	0.992	0.042	0.9	9	8.1	24598
53.329	0.01	0.01	0.9	0.048	0.043	0.996	0.043	0.9	9	8.1	26336
56.932	0.01	0.01	0.9	0.050	0.045	1.000	0.045	0.9	9	8.1	28114
60.616	0.01	0.01	0.9	0.052	0.047	1.004	0.047	0.9	9	8.1	29934
64.380	0.01	0.01	0.9	0.054	0.049	1.008	0.048	0.9	9	8.1	31793
68.223	0.01	0.01	0.9	0.056	0.050	1.012	0.050	0.9	9	8.1	33690
72.142	0.01	0.01	0.9	0.058	0.052	1.016	0.051	0.9	9	8.1	35626
76.136	0.01	0.01	0.9	0.060	0.054	1.020	0.053	0.9	9	8.1	37598
80.203	0.01	0.01	0.9	0.062	0.056	1.024	0.054	0.9	9	8.1	39606
84.342	0.01	0.01	0.9	0.064	0.058	1.028	0.056	0.9	9	8.1	41650
88.550	0.01	0.01	0.9	0.066	0.059	1.032	0.058	0.9	9	8.1	43729
92.828	0.01	0.01	0.9	0.068	0.061	1.036	0.059	0.9	9	8.1	45841
97.173	0.01	0.01	0.9	0.070	0.063	1.040	0.061	0.9	9	8.1	47987
101.584	0.01	0.01	0.9	0.072	0.065	1.044	0.062	0.9	9	8.1	50165
106.059	0.01	0.01	0.9	0.074	0.067	1.048	0.064	0.9	9	8.1	52375
110.599	0.01	0.01	0.9	0.076	0.068	1.052	0.065	0.9	9	8.1	54617
115.200	0.01	0.01	0.9	0.078	0.070	1.056	0.066	0.9	9	8.1	56889
119.863	0.01	0.01	0.9	0.080	0.072	1.060	0.068	0.9	9	8.1	59191
124.585	0.01	0.01	0.9	0.082	0.074	1.064	0.069	0.9	9	8.1	61524
129.367	0.01	0.01	0.9	0.084	0.076	1.068	0.071	0.9	9	8.1	63885
134.206	0.01	0.01	0.9	0.086	0.077	1.072	0.072	0.9	9	8.1	66275
139.102	0.01	0.01	0.9	0.088	0.079	1.076	0.074	0.9	9	8.1	68692
144.054	0.01	0.01	0.9	0.090	0.081	1.080	0.075	0.9	9	8.1	71138
149.061	0.01	0.01	0.9	0.092	0.083	1.084	0.076	0.9	9	8.1	73610
154.122	0.01	0.01	0.9	0.094	0.085	1.088	0.078	0.9	9	8.1	76110
159.236	0.01	0.01	0.9	0.096	0.086	1.092	0.079	0.9	9	8.1	78635
164.402	0.01	0.01	0.9	0.098	0.088	1.096	0.080	0.9	9	8.1	81186
169.619	0.01	0.01	0.9	0.100	0.090	1.100	0.082	0.9	9	8.1	83763

Table A.5 Channel Capacity for S=0.02

Q 10⁻³m³/s	S	n	w (m)	y (m)	A (m²)	P	R	C	L (m)	Flow Area (m²)	I (mm/hour)
0.403	0.02	0.01	0.9	0.002	0.002	0.904	0.002	0.9	9	8.1	199
1.275	0.02	0.01	0.9	0.004	0.004	0.908	0.004	0.9	9	8.1	630
2.499	0.02	0.01	0.9	0.006	0.005	0.912	0.006	0.9	9	8.1	1234
4.025	0.02	0.01	0.9	0.008	0.007	0.916	0.008	0.9	9	8.1	1988
5.822	0.02	0.01	0.9	0.010	0.009	0.920	0.010	0.9	9	8.1	2875
7.866	0.02	0.01	0.9	0.012	0.011	0.924	0.012	0.9	9	8.1	3885
10.141	0.02	0.01	0.9	0.014	0.013	0.928	0.014	0.9	9	8.1	5008
12.633	0.02	0.01	0.9	0.016	0.014	0.932	0.015	0.9	9	8.1	6239
15.329	0.02	0.01	0.9	0.018	0.016	0.936	0.017	0.9	9	8.1	7570
18.220	0.02	0.01	0.9	0.020	0.018	0.940	0.019	0.9	9	8.1	8998
21.297	0.02	0.01	0.9	0.022	0.020	0.944	0.021	0.9	9	8.1	10517
24.551	0.02	0.01	0.9	0.024	0.022	0.948	0.023	0.9	9	8.1	12124
27.976	0.02	0.01	0.9	0.026	0.023	0.952	0.025	0.9	9	8.1	13815
31.565	0.02	0.01	0.9	0.028	0.025	0.956	0.026	0.9	9	8.1	15588
35.313	0.02	0.01	0.9	0.030	0.027	0.960	0.028	0.9	9	8.1	17439
39.215	0.02	0.01	0.9	0.032	0.029	0.964	0.030	0.9	9	8.1	19365
43.265	0.02	0.01	0.9	0.034	0.031	0.968	0.032	0.9	9	8.1	21365
47.458	0.02	0.01	0.9	0.036	0.032	0.972	0.033	0.9	9	8.1	23436
51.792	0.02	0.01	0.9	0.038	0.034	0.976	0.035	0.9	9	8.1	25576
56.260	0.02	0.01	0.9	0.040	0.036	0.980	0.037	0.9	9	8.1	27783
60.861	0.02	0.01	0.9	0.042	0.038	0.984	0.038	0.9	9	8.1	30055
65.590	0.02	0.01	0.9	0.044	0.040	0.988	0.040	0.9	9	8.1	32390
70.444	0.02	0.01	0.9	0.046	0.041	0.992	0.042	0.9	9	8.1	34787
75.419	0.02	0.01	0.9	0.048	0.043	0.996	0.043	0.9	9	8.1	37244
80.514	0.02	0.01	0.9	0.050	0.045	1.000	0.045	0.9	9	8.1	39760
85.724	0.02	0.01	0.9	0.052	0.047	1.004	0.047	0.9	9	8.1	42333
91.048	0.02	0.01	0.9	0.054	0.049	1.008	0.048	0.9	9	8.1	44962
96.482	0.02	0.01	0.9	0.056	0.050	1.012	0.050	0.9	9	8.1	47645
102.024	0.02	0.01	0.9	0.058	0.052	1.016	0.051	0.9	9	8.1	50382
107.672	0.02	0.01	0.9	0.060	0.054	1.020	0.053	0.9	9	8.1	53172
113.424	0.02	0.01	0.9	0.062	0.056	1.024	0.054	0.9	9	8.1	56012
119.277	0.02	0.01	0.9	0.064	0.058	1.028	0.056	0.9	9	8.1	58902
125.229	0.02	0.01	0.9	0.066	0.059	1.032	0.058	0.9	9	8.1	61842
131.279	0.02	0.01	0.9	0.068	0.061	1.036	0.059	0.9	9	8.1	64829
137.423	0.02	0.01	0.9	0.070	0.063	1.040	0.061	0.9	9	8.1	67863
143.661	0.02	0.01	0.9	0.072	0.065	1.044	0.062	0.9	9	8.1	70944
149.991	0.02	0.01	0.9	0.074	0.067	1.048	0.064	0.9	9	8.1	74070
156.410	0.02	0.01	0.9	0.076	0.068	1.052	0.065	0.9	9	8.1	77240
162.917	0.02	0.01	0.9	0.078	0.070	1.056	0.066	0.9	9	8.1	80453
169.511	0.02	0.01	0.9	0.080	0.072	1.060	0.068	0.9	9	8.1	83709
176.190	0.02	0.01	0.9	0.082	0.074	1.064	0.069	0.9	9	8.1	87007
182.952	0.02	0.01	0.9	0.084	0.076	1.068	0.071	0.9	9	8.1	90347
189.796	0.02	0.01	0.9	0.086	0.077	1.072	0.072	0.9	9	8.1	93726
196.720	0.02	0.01	0.9	0.088	0.079	1.076	0.074	0.9	9	8.1	97146
203.723	0.02	0.01	0.9	0.090	0.081	1.080	0.075	0.9	9	8.1	100604
210.804	0.02	0.01	0.9	0.092	0.083	1.084	0.076	0.9	9	8.1	104101
217.961	0.02	0.01	0.9	0.094	0.085	1.088	0.078	0.9	9	8.1	107635
225.194	0.02	0.01	0.9	0.096	0.086	1.092	0.079	0.9	9	8.1	111207
232.500	0.02	0.01	0.9	0.098	0.088	1.096	0.080	0.9	9	8.1	114815
239.878	0.02	0.01	0.9	0.100	0.090	1.100	0.082	0.9	9	8.1	118458

Table A.6 Channel Capacity for S=0.04

Q 10⁻³m³/s	S	n	w (m)	y (m)	A (m²)	P	R	C	L (m)	Flow Area (m²)	I (mm/hour)
0.570	0.04	0.01	0.9	0.002	0.002	0.904	0.002	0.9	9	8.1	281
1.804	0.04	0.01	0.9	0.004	0.004	0.908	0.004	0.9	9	8.1	891
3.535	0.04	0.01	0.9	0.006	0.005	0.912	0.006	0.9	9	8.1	1746
5.693	0.04	0.01	0.9	0.008	0.007	0.916	0.008	0.9	9	8.1	2811
8.233	0.04	0.01	0.9	0.010	0.009	0.920	0.010	0.9	9	8.1	4066
11.125	0.04	0.01	0.9	0.012	0.011	0.924	0.012	0.9	9	8.1	5494
14.342	0.04	0.01	0.9	0.014	0.013	0.928	0.014	0.9	9	8.1	7083
17.866	0.04	0.01	0.9	0.016	0.014	0.932	0.015	0.9	9	8.1	8823
21.679	0.04	0.01	0.9	0.018	0.016	0.936	0.017	0.9	9	8.1	10706
25.767	0.04	0.01	0.9	0.020	0.018	0.940	0.019	0.9	9	8.1	12724
30.118	0.04	0.01	0.9	0.022	0.020	0.944	0.021	0.9	9	8.1	14873
34.720	0.04	0.01	0.9	0.024	0.022	0.948	0.023	0.9	9	8.1	17146
39.564	0.04	0.01	0.9	0.026	0.023	0.952	0.025	0.9	9	8.1	19538
44.640	0.04	0.01	0.9	0.028	0.025	0.956	0.026	0.9	9	8.1	22045
49.941	0.04	0.01	0.9	0.030	0.027	0.960	0.028	0.9	9	8.1	24662
55.458	0.04	0.01	0.9	0.032	0.029	0.964	0.030	0.9	9	8.1	27387
61.186	0.04	0.01	0.9	0.034	0.031	0.968	0.032	0.9	9	8.1	30215
67.116	0.04	0.01	0.9	0.036	0.032	0.972	0.033	0.9	9	8.1	33144
73.244	0.04	0.01	0.9	0.038	0.034	0.976	0.035	0.9	9	8.1	36170
79.564	0.04	0.01	0.9	0.040	0.036	0.980	0.037	0.9	9	8.1	39291
86.070	0.04	0.01	0.9	0.042	0.038	0.984	0.038	0.9	9	8.1	42504
92.758	0.04	0.01	0.9	0.044	0.040	0.988	0.040	0.9	9	8.1	45806
99.622	0.04	0.01	0.9	0.046	0.041	0.992	0.042	0.9	9	8.1	49196
106.659	0.04	0.01	0.9	0.048	0.043	0.996	0.043	0.9	9	8.1	52671
113.863	0.04	0.01	0.9	0.050	0.045	1.000	0.045	0.9	9	8.1	56229
121.232	0.04	0.01	0.9	0.052	0.047	1.004	0.047	0.9	9	8.1	59868
128.761	0.04	0.01	0.9	0.054	0.049	1.008	0.048	0.9	9	8.1	63586
136.446	0.04	0.01	0.9	0.056	0.050	1.012	0.050	0.9	9	8.1	67381
144.284	0.04	0.01	0.9	0.058	0.052	1.016	0.051	0.9	9	8.1	71251
152.272	0.04	0.01	0.9	0.060	0.054	1.020	0.053	0.9	9	8.1	75196
160.406	0.04	0.01	0.9	0.062	0.056	1.024	0.054	0.9	9	8.1	79213
168.683	0.04	0.01	0.9	0.064	0.058	1.028	0.056	0.9	9	8.1	83300
177.101	0.04	0.01	0.9	0.066	0.059	1.032	0.058	0.9	9	8.1	87457
185.656	0.04	0.01	0.9	0.068	0.061	1.036	0.059	0.9	9	8.1	91682
194.346	0.04	0.01	0.9	0.070	0.063	1.040	0.061	0.9	9	8.1	95973
203.168	0.04	0.01	0.9	0.072	0.065	1.044	0.062	0.9	9	8.1	100330
212.119	0.04	0.01	0.9	0.074	0.067	1.048	0.064	0.9	9	8.1	104750
221.197	0.04	0.01	0.9	0.076	0.068	1.052	0.065	0.9	9	8.1	109233
230.400	0.04	0.01	0.9	0.078	0.070	1.056	0.066	0.9	9	8.1	113778
239.725	0.04	0.01	0.9	0.080	0.072	1.060	0.068	0.9	9	8.1	118383
249.170	0.04	0.01	0.9	0.082	0.074	1.064	0.069	0.9	9	8.1	123047
258.733	0.04	0.01	0.9	0.084	0.076	1.068	0.071	0.9	9	8.1	127769
268.412	0.04	0.01	0.9	0.086	0.077	1.072	0.072	0.9	9	8.1	132549
278.204	0.04	0.01	0.9	0.088	0.079	1.076	0.074	0.9	9	8.1	137385
288.108	0.04	0.01	0.9	0.090	0.081	1.080	0.075	0.9	9	8.1	142276
298.122	0.04	0.01	0.9	0.092	0.083	1.084	0.076	0.9	9	8.1	147221
308.244	0.04	0.01	0.9	0.094	0.085	1.088	0.078	0.9	9	8.1	152219
318.472	0.04	0.01	0.9	0.096	0.086	1.092	0.079	0.9	9	8.1	157270
328.804	0.04	0.01	0.9	0.098	0.088	1.096	0.080	0.9	9	8.1	162372
339.239	0.04	0.01	0.9	0.100	0.090	1.100	0.082	0.9	9	8.1	167525

APPENDIX B

UNCERTAINTY ANALYSIS OF EXPERIMENTAL DATA

An accepted principle in engineering is that all measurements have errors. By taking this principle into consideration, uncertainty analysis was performed for Q, E, and Fr values by using the following basic definitions;

$$\delta R = \left\{ \sum_1^n \left((\partial R / \partial x_i) \delta x_i \right)^2 \right\}^{1/2} \qquad (B.1)$$

$$\delta R = \left\{ \sum_1^n \left[R(x_i + \delta x_i) - R(x_i) \right]^2 \right\}^{1/2} \qquad (B.2)$$

where R represents the result computed from the n measurands $x_1, \ldots, x_i, \ldots, x_n$. δR is the overall uncertainty interval of R and δx_i is the precision error

B.1 Uncertainty Analysis for Q

In the present study, discharge is calculated by equation B.3;

$$Q = \frac{wL\Delta y}{t} \qquad (B.3)$$

where w is the width of the pool, L is the length of the pool and Δy is the difference in the water height in measured time t. Equation B.3 can be rewritten for intercepted and bypass flow as equations B.4 and B.5 respectively;

$$Q_i = \frac{wL(y_{i2} - y_{i1})}{t} \tag{B.4}$$

$$Q_b = \frac{wL(y_{b2} - y_{b1})}{t} \tag{B.5}$$

where y_{i1} and y_{i2} are the water height measurements in the pool for intercepted flow in a measured time and y_{b1} and y_{b2} are the water height measurements in the pool for bypass flow in a measured time.

As can be seen from equation B.4, Q_i is computed from five measurands; w, L, t, y_{i1} and y_{i2}. In the same way, from equation B.5, Q_b is computed from five measurands; w, L, t, y_{b1} and y_{b2}. Consequently, Equation B.2 can be written for the ΔQ values as follows;

$$\delta\Delta Q = \left\{ \sum_1^n \left[\Delta Q(x_i + \delta x_i) - \Delta Q(x_i) \right]^2 \right\}^{1/2} \tag{B.6}$$

Equation B.4 can be also written as;

$$\delta\Delta Q_i = \left\{ \begin{array}{l} \left(\Delta Q_i(\Delta w + \delta\Delta w) - \Delta Q_i(\Delta w)\right)^2 + \left(\Delta Q_i(\Delta L + \delta\Delta L) - \Delta Q_i(\Delta L)\right)^2 \\ + \left(\Delta Q_i(\Delta t + \delta\Delta t) - \Delta Q_i(\Delta t)\right)^2 + \left(\Delta Q_i(\Delta y_{i1} + \delta\Delta y_{i1}) - \Delta Q_i(\Delta y_{i1})\right)^2 \\ + \left(\Delta Q_i(\Delta y_{i2} + \delta\Delta y_{i2}) - \Delta Q_i(\Delta y_{i2})\right)^2 \end{array} \right\}^{1/2}$$

$$\tag{B.7}$$

In the same way, equation B.5 can also be written as;

$$\delta\Delta Q_b = \left\{ \begin{array}{l} \left(\Delta Q_b(\Delta w + \delta\Delta w) - \Delta Q_b(\Delta w)\right)^2 + \left(\Delta Q_b(\Delta L + \delta\Delta L) - \Delta Q_b(\Delta L)\right)^2 \\ + \left(\Delta Q_b(\Delta t + \delta\Delta t) - \Delta Q_b(\Delta t)\right)^2 + \left(\Delta Q_b(\Delta y_{b1} + \delta\Delta y_{b1}) - \Delta Q_b(\Delta y_{b1})\right)^2 \\ + \left(\Delta Q_b(\Delta y_{b2} + \delta\Delta y_{b2}) - \Delta Q_b(\Delta y_{b2})\right)^2 \end{array} \right\}^{1/2}$$

(B.8)

where $\delta\Delta w$ is the precision error associated with w and equal to ± 0.0005m, $\delta\Delta L$ is the precision error associated with L and equal to ± 0.0005m, $\delta\Delta y_{i1}$ is the precision error associated with y_{i1} and equal to ± 0.0005m, $\delta\Delta y_{i2}$ is the precision error associated with y_{i2} and equal to ± 0.0005m, $\delta\Delta y_{b1}$ is the precision error associated with y_{b1} and equal to ± 0.0005m, $\delta\Delta y_{b2}$ is the precision error associated with y_{b2} and equal to ± 0.0005m and $\delta\Delta t$ is the precision error associated with t and equal to ± 0.2s.

Uncertainty values computed by using equation B.7 for Q_i are listed in Table B.1 and plotted in Figure B.1.

Table B.1 Uncertainty values for Q_i

ΔQ_i (10^{-3} m^3/s)	$\delta\Delta Q_i$ (10^{-3} m^3/s)	%($\delta\Delta Q_i/\Delta Q_i$)
0.121	0.003	2.832
0.139	0.004	2.833
0.227	0.006	2.836
0.228	0.005	2.364
0.286	0.005	1.777
0.305	0.003	1.019
0.504	0.007	1.433
0.594	0.005	0.903
0.599	0.006	1.031
0.626	0.009	1.441
0.729	0.005	0.730
0.737	0.009	1.210
0.878	0.011	1.220
0.901	0.003	0.363
1.004	0.007	0.744
1.027	0.008	0.745
1.189	0.009	0.755
1.221	0.006	0.453
1.559	0.009	0.564
1.664	0.005	0.309
1.839	0.008	0.414
2.264	0.012	0.508
2.339	0.020	0.861
2.507	0.010	0.411
2.524	0.019	0.738
2.563	0.012	0.453
3.760	0.024	0.643
3.810	0.014	0.366
4.015	0.034	0.842
4.288	0.046	1.082
4.906	0.071	1.457
6.499	0.099	1.522
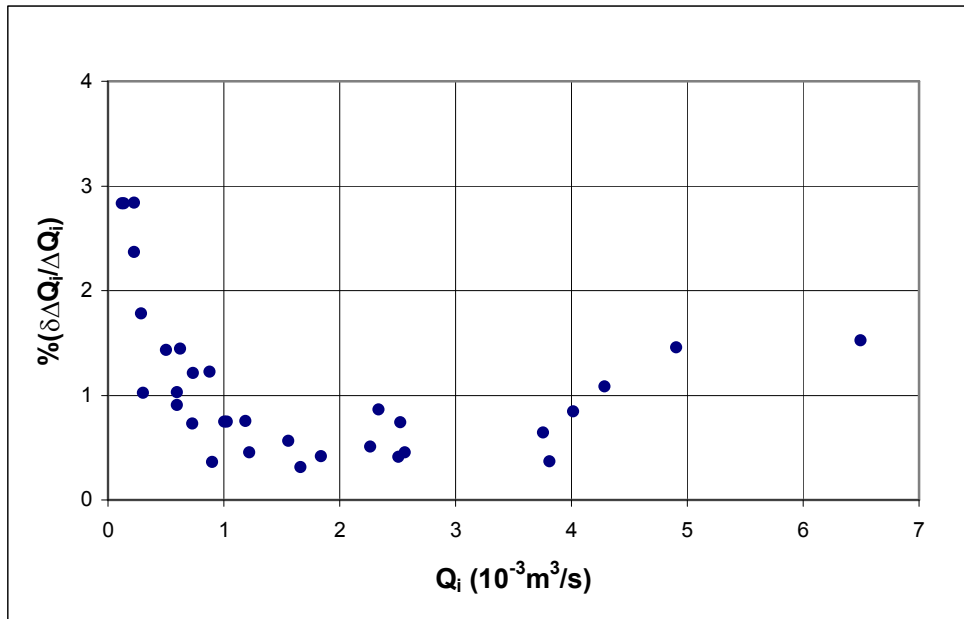
Figure B.1 Uncertainty ratio for Q_i

Uncertainty values computed by using equation B.8 for Q_b are listed in Table B.2 and plotted in Figure B.2.

Table B.2 Uncertainty values for Q_b

ΔQ_b (10^{-3} m^3/s)	$\delta\Delta Q_b$ (10^{-3} m^3/s)	%($\delta\Delta Q_b/\Delta Q_b$)
0.095	0.005	4.717
0.117	0.002	2.024
0.120	0.004	3.539
0.132	0.003	2.361
0.180	0.006	3.542
0.192	0.007	3.543
0.223	0.003	1.293
0.223	0.006	2.836
0.229	0.008	3.545
0.261	0.004	1.422
0.282	0.004	1.423
0.326	0.005	1.424
0.338	0.003	0.894
0.338	0.003	1.020
0.350	0.007	2.033
0.358	0.010	2.846
0.366	0.005	1.426
0.383	0.006	1.584
0.389	0.007	1.782
0.402	0.007	1.783
0.425	0.008	1.784
0.442	0.006	1.430
0.455	0.005	1.024
0.456	0.008	1.786
0.503	0.008	1.492
0.514	0.012	2.385
0.560	0.010	1.794
0.593	0.008	1.411
0.803	0.006	0.733
0.819	0.020	2.425
0.898	0.008	0.919
0.957	0.023	2.449
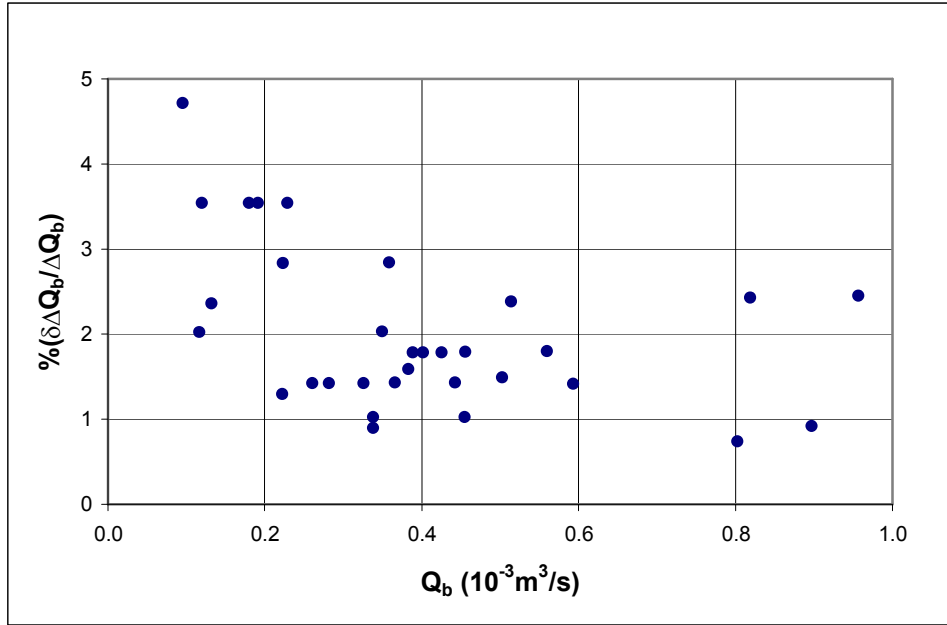
Figure B.2 Uncertainty ratio for Q_b

B.2 Uncertainty Analysis for E

In the present study, E is calculated by equation 2.1;

$$E = \frac{Q_i}{Q_T} \tag{2.1}$$

If equations of Q_i and Q_T are included to equation 2.1;

$$E = \frac{w_i L_i \dfrac{(\Delta y_{i2} - \Delta y_{i1})}{t_i}}{w_i L_i \left(\dfrac{(\Delta y_{i2} - \Delta y_{i1})}{t_i} \right) + w_b L_b \left(\dfrac{(\Delta y_{b2} - \Delta y_{b1})}{t_b} \right)} \tag{B.9}$$

where w_i and L_i are the width and length of the pool for intercepted flow and w_b and L_b are the width and length of the pool for bypass flow, t_i is the time interval for intercepted flow and t_b is the time interval for bypass flow.

As can be seen from equation B.9, E is computed from ten measurands; w_i, L_i, w_b, L_b, y_{i1}, y_{i2}, y_{b1}, y_{b2}, t_i and t_b. Consequently, Equation B.2 can be written for the ΔE values are as follows;

$$\delta\Delta E = \left\{ \begin{array}{l} \left(\Delta E(\Delta w_i + \delta\Delta w_i) - \Delta E(\Delta w_i)\right)^2 + \left(\Delta E(\Delta w_b + \delta\Delta w_b) - \Delta E(\Delta w_b)\right)^2 \\ + \left(\Delta E(\Delta L_i + \delta\Delta L_i) - \Delta E(\Delta L_i)\right)^2 + \left(\Delta E(\Delta L_b + \delta\Delta L_b) - \Delta E(\Delta L_b)\right)^2 \\ + \left(\Delta E(\Delta t_i + \delta\Delta t_i) - \Delta E(\Delta t_i)\right)^2 + \left(\Delta E(\Delta t_b + \delta\Delta t_b) - \Delta E(\Delta t_b)\right)^2 + \\ + \left(\Delta E(\Delta y_{b1} + \delta\Delta y_{b1}) - \Delta E(\Delta y_{b1})\right)^2 + \left(\Delta E(\Delta y_{b2} + \delta\Delta y_{b2}) - \Delta E(\Delta y_{b2})\right)^2 \\ + \left(\Delta E(\Delta y_{i1} + \delta\Delta y_{i1}) - \Delta E(\Delta y_{i1})\right)^2 + \left(\Delta E(\Delta y_{i2} + \delta\Delta y_{i2}) - \Delta E(\Delta y_{i2})\right)^2 \end{array} \right\}^{1/2}$$

(B.10)

where $\delta\Delta w_i$ is the precision error associated with w_i and equal to $\pm 0.0005\text{m}$, $\delta\Delta w_b$ is the precision error associated with w_b and equal to $\pm 0.0005\text{m}$, $\delta\Delta L_i$ is the precision error associated with L_i and equal to $\pm 0.0005\text{m}$, $\delta\Delta L_b$ is the precision error associated with L_b and equal to $\pm 0.0005\text{m}$, $\delta\Delta y_{i1}$ is the precision error associated with y_{i1} and equal to $\pm 0.0005\text{m}$, $\delta\Delta y_{i2}$ is the precision error associated with y_{i2} and equal to $\pm 0.0005\text{m}$, $\delta\Delta y_{b1}$ is the precision error associated with y_{b1} and equal to $\pm 0.0005\text{m}$, $\delta\Delta y_{b2}$ is the precision error associated with y_{b2} and equal to $\pm 0.0005\text{m}$,$\delta\Delta t_i$ is the precision error associated with t_i and equal to $\pm 0.2\text{s}$ and $\delta\Delta t_b$ is the precision error associated with t_b and equal to $\pm 0.2\text{s}$

Uncertainty values computed by using equation B.10 for E are listed in Table B.3 and plotted in Figure B.3.

Table B.3 Uncertainty values for E

ΔE	δΔE	%(δΔE/ΔE)
0.480	0.038	0.253
0.490	0.040	0.375
0.559	0.038	0.408
0.568	0.037	0.888
0.611	0.041	0.158
0.617	0.035	1.014
0.636	0.037	0.218
0.647	0.034	1.586
0.647	0.040	0.177
0.673	0.033	1.095
0.694	0.031	1.446
0.704	0.033	0.322
0.710	0.031	0.403
0.718	0.030	0.425
0.727	0.029	0.817
0.729	0.029	0.822
0.737	0.029	1.615
0.761	0.027	0.958
0.762	0.026	3.366
0.762	0.027	1.183
0.771	0.026	1.138
0.789	0.024	1.547
0.810	0.022	3.117
0.817	0.022	1.909
0.823	0.021	2.842
0.831	0.020	2.002
0.834	0.020	2.205
0.849	0.019	2.666
0.880	0.015	4.273
0.881	0.015	2.845
0.893	0.014	4.265
0.904	0.013	4.743
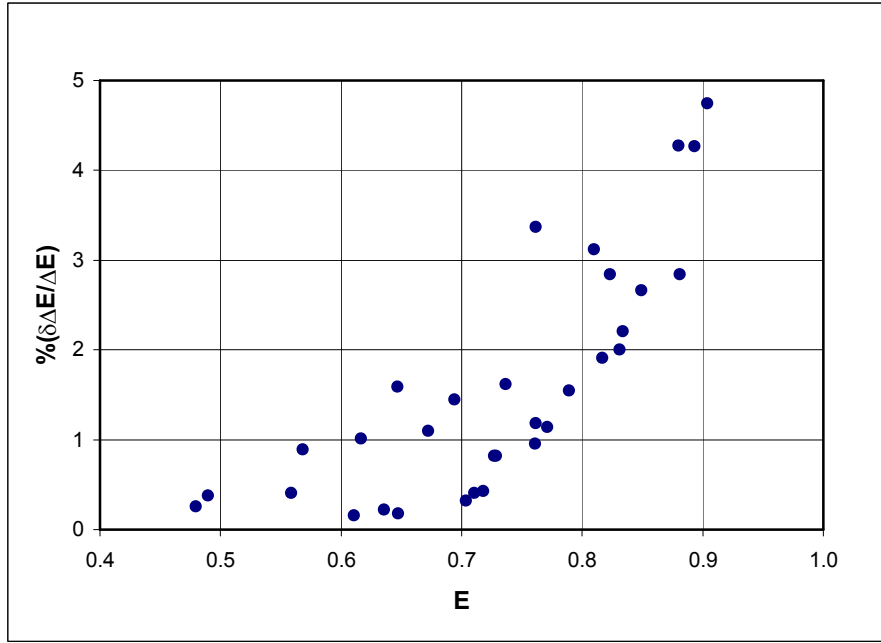
Figure B.3 Uncertainty ratio for E

B.3 Uncertainty Analysis for Fr

In the present study, Fr is calculated by equation B.11;

$$Fr = \frac{Q_T}{\sqrt{9.81w_c{}^2 y_1{}^3}} \tag{B.11}$$

where w_c is the witdh of the channel and y_1 is the water depth in the channel. If equation for Q_T is written explicitly in equation B.11, B.12 is obtained;

$$Fr = \frac{w_i L_i\left(\dfrac{(\Delta y_{i2} - \Delta y_{i1})}{t_i}\right) + w_b L_b\left(\dfrac{(\Delta y_{b2} - \Delta y_{b1})}{t_b}\right)}{\sqrt{9.81w_c{}^2 y_1{}^3}} \tag{B.12}$$

As can be seen from equation B.12, Fr is computed from twelve measurands; w_i, L_i, w_b, L_b, y_{i1}, y_{i2}, y_{b1}, y_{b2}, t_i, t_b, w_c and y_1. Consequently, Equation B.2 can be written for the ΔFr values are as follows;

$$\delta \Delta Fr = \left\{ \begin{array}{l} \left(\Delta Fr\left(\Delta w_i + \delta \Delta w_i\right) - \Delta Fr\left(\Delta w_i\right)\right)^2 + \left(\Delta Fr\left(\Delta w_b + \delta \Delta w_b\right) - \Delta Fr\left(\Delta w_b\right)\right)^2 \\ + \left(\Delta Fr\left(\Delta L_i + \delta \Delta L_i\right) - \Delta Fr\left(\Delta L_i\right)\right)^2 + \left(\Delta Fr\left(\Delta L_b + \delta \Delta L_b\right) - \Delta Fr\left(\Delta L_b\right)\right)^2 \\ + \left(\Delta Fr\left(\Delta t_i + \delta \Delta t_i\right) - \Delta Fr\left(\Delta t_i\right)\right)^2 + \left(\Delta Fr\left(\Delta t_b + \delta \Delta t_b\right) - \Delta Fr\left(\Delta t_b\right)\right)^2 + \\ + \left(\Delta Fr\left(\Delta y_{b1} + \delta \Delta y_{b1}\right) - \Delta Fr\left(\Delta y_{b1}\right)\right)^2 + \left(\Delta Fr\left(\Delta y_{b2} + \delta \Delta y_{b2}\right) - \Delta Fr\left(\Delta y_{b2}\right)\right)^2 \\ + \left(\Delta Fr\left(\Delta y_{i1} + \delta \Delta y_{i1}\right) - \Delta Fr\left(\Delta y_{i1}\right)\right)^2 + \left(\Delta Fr\left(\Delta y_{i2} + \delta \Delta y_{i2}\right) - \Delta Fr\left(\Delta y_{i2}\right)\right)^2 \\ + \left(\Delta Fr\left(\Delta y_1 + \delta \Delta y_1\right) - \Delta Fr\left(\Delta y_1\right)\right)^2 + \left(\Delta Fr\left(\Delta w_c + \delta \Delta w_c\right) - \Delta Fr\left(\Delta w_c\right)\right)^2 \end{array} \right\}^{1/2}$$

(B.13)

where $\delta \Delta w_i$ is the precision error associated with w_i and equal to $\pm 0.0005m$, $\delta \Delta w_b$ is the precision error associated with w_b and equal to $\pm 0.0005m$, $\delta \Delta L_i$ is the precision error associated with L_i and equal to $\pm 0.0005m$, $\delta \Delta L_b$ is the precision error associated with L_b and equal to $\pm 0.0005m$, $\delta \Delta y_{i1}$ is the precision error associated with y_{i1} and equal to $\pm 0.0005m$, $\delta \Delta y_{i2}$ is the precision error associated with y_{i2} and equal to $\pm 0.0005m$, $\delta \Delta y_{b1}$ is the precision error associated with y_{b1} and equal to $\pm 0.0005m$, $\delta \Delta y_{b2}$ is the precision error associated with y_{b2} and equal to $\pm 0.0005m$, $\delta \Delta w_c$ is the precision error associated with w_c and equal to $\pm 0.0005m$, $\delta \Delta y_1$ is the precision error associated with y_1 and equal to $\pm 0.0001m$, $\delta \Delta t_b$ is the precision error associated with t_b and equal to $\pm 0.2s$ and $\delta \Delta t_i$ is the precision error associated with t_i and equal to $\pm 0.2s$.

Uncertainty values computed by using equation B.14 for Fr are listed in Table B.4 and plotted in Figure B.4.

Table B.4 Uncertainty values for Fr

ΔFr	δΔFr	%(δΔFr/ΔFr)
0.4824	0.0048	0.9933
0.6266	0.0151	2.4159
1.1594	0.0452	3.9025
1.5966	0.0689	4.3148
1.7428	0.0771	4.4213
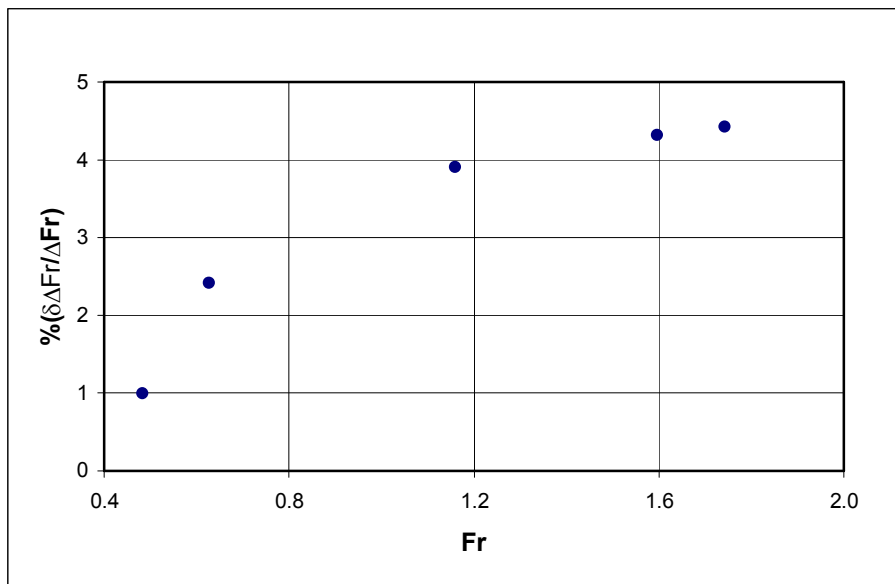
Figure B.4 Uncertainty ratio for Fr

APPENDIX C

DIMENSIONAL ANALYSIS

This study was accomplished as an initiation of a grate inlet setup which will be continued with different variations on this setup. In order to direct the following studies in compliance with this study and to point out the variables affecting the efficiency of the grate inlets, dimensional analysis is performed.

The variables are listed below with their dimensions.

b	: Width of the channel	[L]
E	: Efficiency	[ ]
n	: Manning roughness coefficient	[ ]
Q_i	: Intercepted flow rate	$[L^3/T]$
Q_b	: Bypass flow rate	$[L^3/T]$
Q_t	: Total flow rate	$[L^3/T]$
S	: Slope of the channel	[ ]
y	: Flow depth	[L]
g	: The Acceleration Due to Gravity	$[L/T^2]$
μ	: Viscosity of Fluid	[M/LT]
ρ	: Density of Fluid	$[M/L^3]$
V	: Velocity	[L/T]
D	: Geometric parameter for grate	[L]

So the efficiency will be a function as follows;

$$E = f (b,n,Q_i,Q_b,S,y,g,\mu,\rho,V) \qquad\qquad (C.1)$$

Then the equation C.1 is reduced using Buckingham π theorem using ρ,V and y as repeating variables,

$$E = f (b/y, n, Q/Vy^2, S, Fr, Re, D/y) \qquad\qquad (C.2)$$

If Reynolds effects are neglected and the width of the channel is wide enough not to produce width effects, and in addition Manning's roughness coefficient is dropped as it is held constant during the experiments, the efficiency will be a function of slope, Froude and incoming discharge.

$$E = f (S, Fr) \qquad\qquad (C.3)$$